Note to reader

This draft version of Chapter 4 in the Technical Background Report to the Global Mercury Assessment 2018 is made available for review by national representatives and experts. The draft version contains material that will be further refined and elaborated after the review process. Specific items where the content of this draft chapter will be further improved and modified are:

1. Modelling results based on the new GMA 2018 emissions inventory will be added and sent out for separate review.
2. Introduction will be updated in line with the new modelling results.
3. Internal references to other parts of the GMA report will be updated.
4. Conclusions and main messages will be finalised.

GMA 2018 Draft Chapter 4 Atmospheric Pathways, transport and fate. Oleg Travnikov, Johannes Bieser, Mark Cohen, Ashu Dastoor, Ian Hedgecock, Che-Jen Lin, Noelle Selin and Xun Wang.

8023

8024 # Contents

8042

8043
8044

8045

8046

Chapter 4 Atmospheric pathways

4.1. Introduction

Mercury (Hg) has a long environmental lifetime and cycles between the atmosphere, ocean, and land. Mercury released to the atmosphere can travel globally: it undergoes atmospheric redox reactions, deposits to the Earth's surface, and can continue to cycle between surface and atmosphere for decades to centuries. Using a combination of models and measurement, work since GMA 2013 has addressed aspects of Hg's transport and fate, including emissions, atmospheric chemistry, removal processes, modelling, and historical trends. In addition, a number of other studies have provided additional insights into regional and local mercury cycling.

Emissions and their speciation: The emergence of new regional and global emissions inventories provide alternatives to the UNEP/AMAP inventories for the present day as well as new historical estimates. Uncertainties remain in quantifying emissions, particularly from certain regions and sectors and in mercury speciation.

Atmospheric chemistry: New information has solidified our knowledge about mercury oxidation reactions, including the primary importance of Br chemistry in mercury oxidation. Models including these reactions have shorter mercury lifetimes, and can reproduce some free tropospheric observations. Recent model intercomparisons have shown that there remain challenges in reproducing observed concentrations and patterns in several areas. In particular, uncertainty remains in atmospheric speciation (Jaffe et al., 2014), the potential importance of heterogeneous chemistry (Ariya et al, 2015), and the mechanism and rate of atmospheric reduction reactions (de Foy et al., 2016).

Removal Processes: Wet deposition measurement-model comparisons, in particular in convective storms, have provided insight into the vertical distribution of mercury in the troposphere as well as oxidation processes. Dry deposition remains more poorly quantified than wet deposition, and there remains disagreement among models on its global magnitude. New measurement analyses of dry deposition have shown the importance of gaseous elemental mercury uptake into the terrestrial environment, in addition to deposition of oxidized mercury forms.

Mercury modelling: Recent model development has advanced our ability to simulate Hg transport in the atmosphere between different geographical regions and account for multi-media cycling of Hg, including the importance of legacy Hg (*this paragraph will be updated based on new simulation results)*.

Historical trends and future scenarios: Recent declines have been observed in both atmospheric mercury and wet deposition, on the order of 1-2% per year, that differ by region. Some modelling studies have reproduced these trends, attributing some regional variations to declines in emissions. Observed trends, however, are small compared with uncertainties in surface-atmosphere fluxes, anthropogenic sources, and attributable fraction. Future changes under policy scenarios could reduce mercury deposition in the future; however, the influence of climate change and legacy mercury complicates our ability to assess these potential future changes in models.

4.2. Atmospheric processes

In GMA 2013 the atmospheric chemistry section focussed on emission speciation, atmospheric Hg redox chemistry, the processes governing the exchange of Hg at environmental interfaces and atmospheric Hg dynamics. Since then progress has been made in all key areas of interest regarding atmospheric Hg chemistry and also in some which were not included, although it may seem that more questions have been posed than have been answered. Atmospheric Hg processes have been studied or inferred using theoretical, experimental, monitoring and modelling techniques and more often than not a combination of these. The chemical nature of atmospheric Hg, whether it is elemental, oxidised or bound (tightly or loosely) to atmospheric particulate matter, and its interconversion between these forms, continues to pose a challenge for the emission inventory, modelling and measurement communities alike.

4.2.1. Emissions and their speciation

Other estimates in addition to the AMAP/UNEP emission inventories of 2008 and 2013 (*AMAP/UNEP,* 2008; 2013) are now available. An alternative global anthropogenic emission inventory is available from 1970 (*Muntean et al*., 2014) which uses different approaches to determine emissions from anthropogenic activity sectors, and differs in both Hg emissions total and speciation from the AMAP/UNEP. All-time emissions to the atmosphere have been also developed in combination with estimates of releases (*Streets et al*., 2011; 2017). There have also been improvements to regional inventories (*Rafaj et al*., 2014; *Wu et al*., 2016), to estimates of historical and legacy emissions (*Amos et al.*, 2013; 2015), and also the contribution made by the past and current use of Hg in commercial products (*Horowitz et al*., 2014). A modelling comparison of the influence of using different global emission inventories on worldwide Hg deposition fields was performed recently (*De Simone et al*., 2016).

The importance of accurate emission inventories and how their uncertainty relates to the implementation of the Minamata Convention has been discussed in *Kwon and Selin* (2016). The observed decrease in atmospheric Hg species concentrations (e.g. *Zhou et al*., 2016) has led to some

authors to call into question the accuracy of current emission inventories, particularly in their estimation of European and North American sources (*Zhang et al*., 2016), and suggest that there has been a 20% decrease in total Hg emissions between 1990 and 2010, with a 30% decrease in elemental Hg.

Since GMA 2013 the discussion of emission speciation has continued. Regional and global modelling studies have also called into question the speciation in emission inventories for specific areas (*Kos et al.*, 2013; *Beiser et al*., 2014; *Zhang et al*., 2015). The partitioning of Hg(II) compounds between the gas and particulate phases is still difficult to determine. In part this is due to the lack of information concerning the Hg(II) chemical species present in the atmosphere, but also because of the vast range of particulate chemical composition. *Ariya et al*. (2015) discuss in some detail heterogeneous reactions of Hg and also interactions between Hg and fly ash which is particularly important in combustion processes leading to Hg emissions.

4.2.2. Atmospheric chemistry

Atmospheric redox reactions can occur homogeneously in the gas and aqueous phase, and heterogeneously on the surface of fog/cloud droplets and atmospheric particulate matter. At first sight the homogeneous reactions would appear to be straightforward, while it is clear that the heterogeneous reactions may be somewhat more complex to study due to the very wide range of composition of the surfaces at which reactions may take place. A recent review by *Ariya et al.* (2015) provides an in depth overview of Hg reactions and transformations in environmental media.

Perhaps the major obstacle to understanding the processes by which Hg is oxidised, reduced, adsorbed and desorbed in the atmosphere and both in and on atmospheric particles is the fact that the nature of the oxidised Hg compounds in the atmosphere remains uncertain. While it seems clear that O_3, OH, and Br are all implicated in the oxidation of atmospheric Hg, the precise nature of the reactions occurring and identity (and phase) of the products remains the subject of speculation. Recent theoretical studies have given further insight into the Br initiated oxidation of Hg; this reaction proceeds via an unstable $HgBr^*$ intermediate which may react further or decompose back to Hg and Br (*Goodsite et al.,* 2004, 2012). A series of theoretical studies have investigated the possibility, or not, that $HgBr^*$ may react with a series of small atmospheric compounds (*Dibble et al,* 2012, 2013, 2014; *Jiao and Dibble,* 2015; 2017) and also recently with VOCs (*Dibble and Schwid,* 2017). It now seems likely that the $HgBr^*$ intermediate may react further with the relatively abundant radicals HO_2 and NO_2. Meanwhile the likelihood that elemental Hg is oxidised by molecular halogens has been shown to be improbable and that oxidation to Hg halides requires either halogen atom initiation or the presence of a reactive surface (*Auzmendi-Murua et al*., 2014).

Considering only oxidation reactions can lead to atmospheric lifetimes for elemental Hg which cannot be reconciled with its global distribution and relatively uniform background hemispheric concentrations. Given the experimental and observational (in particular the rapid depletion of elemental Hg concentrations seen during AMDEs) evidence as well as the collaborative results from modelling studies that point to an atmospheric lifetime against oxidation of less than 3 months based on two recent model studies (*Shah et al.,* 2016; *Horowitz et al*., 2017). This is shorter than the estimated overall lifetime of around 12 months (*Schroeder and Munthe*, 1998). There is, therefore, likely to be Hg reduction taking place in the atmosphere, and over the years a number of mechanisms have been suggested, most of which have involved the atmospheric aqueous phase, cloud and fog droplets and deliquesced aerosols, as the reaction medium. A thorough discussion of possible reduction pathways can be found in *Ariya et al*. (2015). Most recently it has been suggested that atmospheric reduction occurs in cloud droplets via the photo-reduction of organic Hg compounds, and a model study using modelled organic aerosol concentrations as an indicator of organic Hg compound concentrations (*Horowitz et al*., 2017), based a regional modelling study which included the reduction of Hg(II) by dicarboxylic acids (*Bash et al.,* 2014). However, it should be pointed out that the rate of reduction in global models is largely tuned to reproduce observed Hg species concentrations.

Further information concerning Hg oxidation at different levels in the atmosphere has been obtained as a result of the increasing amount of observational data available from high-altitude measurement sites, observations combined with modelling can help determine which Hg atmospheric oxidation pathways are more or less likely (see for example *Weiss-Penzias et al*., 2015). In this study it was found that in one high Hg(II) free tropospheric event there was almost quantitative oxidation of Hg(0) to Hg(II). Interestingly a better model reproduction of the observations (using the GEOS-Chem model) was found when employing the O_3/OH rather than the $HgBr^*$ oxidation scheme. However, it should be pointed out that was not the most recent HgBr* scheme as described in (*Horowitz et al*., 2017). Recent model-measurement comparisons have shown episodes of high oxidized mercury concentrations that can be explained by Br oxidation (*Coburn et al.,* 2016; *Gratz et al*., 2015), and that this is consistent with constraints from global biogeochemical cycling (*Shah et al.*, 2016). These studies collectively show that measurements in free tropospheric air can significantly aid understanding of the atmospheric chemistry and dynamics of Hg. Uncertainties in measuring oxidized mercury (*Jaffe et al.,* 2014), however, challenge our ability to further advance model-measurement comparison of mercury species (*Gustin et al*., 2015).

Kos et al. (2013) performed a detailed analysis of the uncertainties associated with Hg(II) measurement and modelling. A number of model sensitivity runs were carried out to evaluate different chemical mechanisms and speciation of anthropogenic Hg emissions. In particular, they found evident inconsistencies between the emission speciation in existing emission inventories and the measured Hg(II) concentration in surface air. Besides, the OH oxidation chemistry provided better agreement with observations at simulation of the seasonal cycle of wet deposition in North America.

A complex analysis of the major Hg oxidation mechanisms was carried out by *Travnikov et al.* (2017) involving both measured data from ground-based sites and simulation results from four global chemical transport models. It was shown that the Br oxidation mechanism can reproduce successfully the observed seasonal variation of the Hg(II)/Hg(0) ratio in the near-surface air, but it predicts a wet deposition maximum in spring instead of in summer as observed at monitoring sites in North America and Europe. Model runs with OH chemistry correctly simulate both the periods of maximum and minimum values and the amplitude of observed seasonal variation but shift the maximum Hg(II)/Hg(0) ratios from spring to summer. O_3 chemistry does not predict significant seasonal variation of Hg oxidation. The possibility of more complex chemistry and/or multiple Hg oxidation pathways occurring concurrently in various parts of the atmosphere was suggested.

Bieser et al. (2017) used the same model ensemble and variety of aircraft observations to study vertical and hemispheric distributions of atmospheric Hg. They also found that different chemical mechanisms were better at reproducing observed Hg(II) patterns depending on altitude. Increased Hg(II) concentrations above the planetary boundary layer in spring and summer could only be reproduced by models using O_3 and OH chemistry. On the other hand, the Br oxidation mechanism allowed to better agreement with observed intercontinental gradients of total Hg in the upper troposphere.

4.2.3. Removal process

Hg removal from the atmosphere occurs via wet and dry deposition. Studies of Hg deposition are providing insights into atmospheric oxidation through the study of Hg in precipitation according to precipitation type (*Dvonch et al., 2005; Holmes et al*., 2016; *Kaulfus et al*., 2017). These studies show that precipitation system morphology influences Hg deposition, with convective systems showing enhanced Hg deposition by a factor of 1.6, season and region also influence the deposition. However, the nature of the precipitation system is of interest as convective systems scavenge Hg from much higher than stratiform systems. Thus indirectly these studies provide information regarding the atmospheric oxidation of Hg because the scavenging height of different cloud types differ

8209 significantly and combined with information on the vertical distribution of potential Hg oxidants,
8210 modelling studies can help to evaluate possible, probable and unlikely oxidation mechanisms at
8211 varying levels in the troposphere. This does of course require the models to more or less accurately
8212 reproduce precipitation system morphologies. More sites measuring Hg in precipitation would clearly
8213 help estimate ecosystem deposition fluxes and refine models.

8214 *Nair et al.* (2013) carried out cloud-resolving simulations of Hg wet deposition processes in several
8215 case studies in the Northeastern and Southeastern U.S. This study is of particular interest as many
8216 modelling simulations have tended to underpredict Hg wet deposition in the Southeastern U.S. It was
8217 found that wet deposition in typical Northeastern thunderstorms would generally be less than
8218 comparable storms in the Southeast – assuming identical atmospheric concentrations of Hg – due to
8219 difference in typical cloud dynamics between the two regions. In addition, it was found that
8220 stratiform precipitation typically only scavenges Hg from the lowest ~4 km of the atmosphere, while
8221 Southeastern thunderstorms can scavenge Hg up to ~10 km.

8222 In another wet deposition process analysis, apparent scavenging ratios, based on ground-level
8223 measurements of speciated air concentrations of Hg and total Hg in precipitation, were studied at
8224 four sites in the Northeastern U.S. (*Huang et al*., 2013). While the use of ground-based
8225 measurements introduced inherent uncertainties, the authors suggested that GOM concentrations
8226 may be underestimated by current measurements, as scavenging ratios based on existing GOM
8227 measurements appeared anomalously high.

8228 Several studies investigated Hg dry deposition processes. *Zhang et al.* (2012) compared CMAQ and
8229 GRAHM modelled dry deposition against field measurements in the Great Lakes region for 2002 and
8230 in some cases, for 2005. Dry deposition from the different models varied by as much as a factor of 2
8231 at regional scales, and larger variations were found at local scales. The authors suggested that the
8232 model-estimated dry deposition values were upper estimates given the tendency of the models to
8233 produce atmospheric concentrations of GOM and PBM significantly greater than measured
8234 concentrations. Following a proposed methodology to estimate bidirectional GEM surface exchange
8235 (*Wright and Zhang*, 2015) dry deposition of Hg was estimated at 24 measurement sites in the U.S.
8236 and Canada (*Zhang et al*., 2016). In this analysis, the dry deposition flux of GEM was estimated to be
8237 significantly larger than that of GOM or PBM at most of the sites. Importance of GEM dry deposition
8238 was also supported by Obrist et al. (2017) who showed that most of the Hg (about 70%) in the
8239 interior Arctic tundra is derived from GEM deposition, with only minor contributions from the
8240 deposition of Hg(II) from precipitation or AMDEs. Additional work is required to reconcile these
8241 results with those of many fate-and-transport models (e.g., *Selin et al*., 2007; *Holmes et al.,* 2010; *Lei*

et al., 2013; *Song et al*., 2015; *Cohen et al*., 2016) and estimates based on field measurement surveys (e.g., *Pirrone et al*., 2010; *Denkenberger et al*., 2012; *Eckley et al.,* 2016) that suggest that the overall net flux of GEM from terrestrial surfaces is upward.

Another aspect of Hg removal from the atmosphere has been studied by a number of groups and is the subject of ongoing monitoring, and that is the deposition of Hg via litterfall, forest canopies seem to be effective sinks for both particulate and oxidised Hg (*Fu et al*., 2016, *Wang et al*., 2016, *Wright et al*. 2016).

4.3. Global mercury atmospheric transport and fate modelling

4.3.1. Overview of recent modelling studies

Since GMA 2013 and GMA Update 2015 a number of modelling studies have addressed the problem of Hg dispersion and fate on a global scale. Global chemical transport models were used for simulations of Hg atmospheric transport, source apportionment of Hg deposition in various geographical regions, and study of processes governing Hg cycling in the atmosphere.

Transport and deposition of Hg on a global scale was studied with the global climate-chemistry model CAM-Chem/Hg for current (*Lei et al*., 2013) and future (*Lei et al*., 2014) conditions. The model generally reproduced global observed TGM levels but overestimated concentrations in South Africa which was explained by the effect of emissions. The analysis also revealed predominant influence of precipitation on the wet deposition pattern. Sensitivity experiments showed that around 22% of total Hg deposition in the United States resulted from domestic anthropogenic sources, and only 9% was contributed by transpacific transport from Asia.

A newly developed global nested GNAQPMS-Hg model was applied for simulations of Hg concentration and deposition levels and evaluation of trans-boundary transport of Chinese anthropogenic emissions (*Chen et al*., 2015). It was shown that Hg emitted from Chinese sources accounts for 62% of total deposition over the country. Contribution of Chinese anthropogenic emissions to deposition over neighbouring regions varies from 15.2% for the Korean Peninsula to 5.9% for Japan. However, for remote regions, such as North America and Europe, the contributions from China do not exceed 5%.

Dastoor et al. (2015) analysed the sources of Hg in the Canadian Arctic with the GRAHM chemical transport model. They found that the total contribution from Hg emissions originating in East Asia to annual Hg deposition in Canadian Arctic (26 to 28%) is more than twice that of the next biggest contributors, the U.S. (7 to 9%) and Europe (6 to 7%), in 2005. Global anthropogenic emissions,

terrestrial emissions, and oceanic emissions were simulated to contribute approximately 30%, 40% and 30% of Hg deposition in the Canadian Arctic, respectively.

A comprehensive analysis of source-receptor relationships of Hg concentration and deposition on a global scale was performed by *Chen et al.* (2014) using the global GEOS-Chem model. It was found that global natural sources are the main contributors for Hg deposition over all regions except East Asia. Deposition over East Asia is dominated by anthropogenic emissions with relative contribution of domestic sources of 50%. Besides, 16% of Hg deposition over North America originates from East Asia, indicating that transpacific transport of East Asian emissions is the major foreign source of Hg deposition in North America. Europe, Southeast Asia, and the Indian subcontinent also make significant contributions to Hg deposition in some receptor regions.

GEOS-Chem was also used by Song et al. (2015) for inverse modelling aimed at constraining present-day atmospheric Hg emissions and relevant physiochemical parameters. Based on the inversion results the authors updated the global estimate of Hg emission from the ocean and terrestrial ecosystems as well as anthropogenic emissions from Asian sources. Re-evaluation of the Hg long-term global biogeochemical cycle showed that legacy Hg becomes more likely to reside in the terrestrial ecosystems than in the ocean. The same model was used by *Shah et al.* (2016) to interpret aircraft measurements and to place new constraints on Hg chemistry in the free troposphere. They found that standard model simulations significantly underestimated observed reactive Hg and that use of faster oxidation mechanism could improve agreement with observations. Recently, the GEOS-Chem model was updated by implementing a new mechanism for atmospheric Hg redox chemistry to gain new insights into the global Hg budget and the patterns of Hg deposition (*Horowitz et al*., 2017).

A new global, Eulerian version of the HYSPLIT-Hg model was applied to simulate global atmospheric transport and deposition of Hg to the Great Lakes (*Cohen et al.*, 2016). The objective of the study was to estimate the amount and source-attribution for atmospheric Hg deposition to each lake, information needed to prioritize amelioration efforts. As shown, the contribution of U.S. direct anthropogenic emissions to total Hg deposition varied from 46% to 11% for different lakes. On average, the U.S. was the largest contributor for Hg deposition to the Great lakes, followed by China, contributing 25% and 6%, respectively. The results of the study also illustrated the importance of atmospheric chemistry, emissions strength, speciation, and proximity, to the amount and source-attribution of Hg deposition.

A number of modelling studies were performed with the global ECHMERIT model addressing impacts of different Hg oxidation mechanisms on the model performance when simulating Hg concentration

and deposition patterns (*De Simone et al*., 2014), contribution of biomass burning to Hg deposition worldwide (*De Simone et al*., 2015), and uncertainties associated with utilizing different global Hg emissions inventories for simulations of Hg atmospheric dispersion (*De Simone et al*., 2016). In particular, it was found that the net effect of biomass burning is to liberate Hg from lower latitudes and disperse it towards higher latitudes where it is eventually deposited. Anthropogenic Hg emissions contribute 20-25% to present-day Hg deposition and roughly two-thirds of primary anthropogenic Hg is deposited to the world's ocean.

An ensemble of four global chemical transport models for Hg (GLEMOS, GEOS-Chem, GEM-MACH-Hg, and ECHMERIT) was recently used in a series of modelling studies focused on assessment of Hg levels over the globe and evaluation of model performance in different geographical regions (*Angot et al*., 2016; *Travnikov et al*., 2017; *Bieser et al*., 2017). *Travnikov et al.* (2017) performed analysis of spatial and temporal variations of Hg surface concentrations and deposition fluxes as well as key processes governing Hg dispersion in the atmosphere. Vertical and interhemispheric distributions and speciation of Hg from the planetary boundary layer to the lower stratosphere were studied by *Bieser et al.* (2017). *Angot et al*. (2016) provided a combined analysis of the model simulations and atmospheric Hg monitoring data in the Arctic and Antarctica.

Many of the above mentioned modelling studies were focussed on assessing source-receptor relationships i.e. how emissions in one region or country contribute to deposition in others. These assessments are based on emission inventories describing current anthropogenic emissions. All models also include estimates of emissions from natural surfaces. These emissions are a mixture of natural emissions and re-emissions of anthropogenic Hg previously emitted from anthropogenic activities in previous years. The anthropogenic contributions to the re-emissions from natural surfaces can originate from both recent deposition (e.g. within 10 years) but also contains contributions from considerably longer time periods (decades to centuries). The percentage contribution of deposition from one region to the other represents the current anthropogenic emissions only.

GMA 2013 noted that multi-compartment modelling of Hg, taking into account the dynamic coupling of atmospheric Hg with the upper ocean and parts of the lithosphere, had advanced over the previous four to five years (*Selin et al*., 2008; *Sunderland et al*., 2009; *Smith-Downey et al*., 2010). Of the models used in the 2015 update, two (GLEMOS and GMHG) were mainly atmospheric models, and one (GEOS-Chem) simulated dynamic cycling. Recent work has advanced observational constraints on Hg biogeochemical cycling, using worldwide measurements (*Agnan et al*., 2016; *Lamborg et al.*, 2014; *Wang et al*., 2016) as well as inverse modelling (*Song et al*., 2015). A key

conclusion of these studies, taken together, is that legacy emissions from land may be smaller than previously assumed in global models. Further multimedia analyses have added to our understanding of the anthropogenic enrichment of the global biogeochemical cycle of Hg (*Amos et al*., 2015), and in particular the role of legacy Hg. See also discussion below in Section 4.4.

4.3.2. Mercury atmospheric loads to terrestrial and aquatic regions

(To be added based on new simulation results)

4.3.3. Source apportionment of mercury deposition

(To be added based on new simulation results)

4.3.4. Contribution of different emission sectors to mercury deposition

(To be added based on new simulation results)

4.4. Historical trends and future scenarios

Evaluation of historical changes of Hg atmospheric concentration and deposition to other environmental media is important because it helps understanding how legacy of previous anthropogenic emissions affects the present-day Hg pollution levels and future environmental responses to expected emission control measures. Human disturbance of Hg natural cycling in the environment by mining and industrial activities led to significant enrichment of atmospheric Hg since pre-industrial times (e.g. *Fitzgerald et al.,* 1998; *Lindberg et al*., 2007; *Biester et al*., 2007). Recently, *Amos et al*. (2013; 2014; 2015) applied a multi-media box model coupling the atmosphere, ocean, and terrestrial reservoirs to reconstruct Hg historical cycling among the geochemical reservoirs on the millennium scale. They found that the present-day atmospheric deposition has increased by a factor of 2.6 from the preindustrial period (ca. 1850), which consistent with sediment archives. Moreover, all-time anthropogenic emissions (ca. since 2000 BC) have enriched the present-day Hg levels in the atmosphere, surface ocean, and deep ocean by factors of 7.5, 5.9, and 2.1, respectively, relative to natural conditions (*Amos et al*., 2013). Besides, *Amos et al*. (2014) showed that accounting for the additional loss of Hg to ocean margin sediments suggests twice as large as the all-time relative enrichment in surface reservoirs. Both model simulations and natural archives provide evidence for peak atmospheric Hg concentrations during the second half of the 20th century and declines in more recent decades (*Amos et al*., 2015).

Changes of Hg atmospheric deposition over two last decades in different geographical regions were evaluated in a number of recent modelling studies. Long-term trends of Hg deposition in Europe were analysed within the framework of the Task Force on Measurements and Modelling under the EMEP Co-operative Programme for Monitoring and Evaluation of the Long-range Transmission of Air

Pollutants in Europe (*Colette et al*., 2016). According to the modelling results presented in the study Hg total deposition in the considered EMEP region (Europe and Central Asia) decreased on average by 23% during the period 1990-2012 (about -1% y^{-1}). However, the deposition trend was essentially non-linear with the rates of deposition reduction being higher at the beginning and lower at the end of the period. Besides, the deposition changes differ significantly between individual countries ranging from 70% decrease to 10% increase in some countries. Generally, the decrease of deposition was larger in the European Union (35% for the period 1990-2012 or -1.5% y^{-1}) than in other parts of the region. Similar rates (-1.5±0.7% y^{-1}) of Hg wet deposition reduction at a number of monitoring sites in Western Europe were simulated for the period 1996-2008 (*Muntean et al*., 2014), which was twice as lower as the observed trend at these sites. *Zhang et al.* (2016) estimated somewhat steeper trend of Hg wet deposition in the same region (-2.0±0.14% y^{-1}). *Muntean et al*. (2014) estimated Hg wet deposition decline in North America as of -2.4±0.7 % y^{-1} for the period 1996-2008. *Zhang et al*. (2016) utilized an updated emissions inventory and obtained somewhat smaller decline -1.4±0.1 % y^{-1} for longer period (1996-2013) in the same region.

Soerensen et al. (2012) used a global Hg model (GEOS-Chem) that coupled the atmosphere, soil, and the surface ocean to analyse a long-term decline in Hg^0 concentration over the Northern Atlantic. They found that existing inventories of Hg anthropogenic emissions cannot explain substantial decrease of observed Hg^0 concentration (-2.5% y^{-1}) for the period 1990-2009 since significant emissions reduction in North America and Europe are balanced by the rise of Hg emissions in East Asia. The model application allowed attributing this decrease to reduction of Hg emissions from the ocean as a result of declining subsurface seawater Hg concentrations. It was hypothesized that the declining trend can be explained by decreased riverine and wastewater inputs at ocean margins (*Soerensen et al*., 2012). However, later *Amos et al*. (2014) showed that the inputs of Hg to the North Atlantic from rivers also did not contribute substantially to these changes. On the other hand, *Zhang et al.* (2016) demonstrated that revised anthropogenic emissions can explain the observed decline in Hg concentration over the past two decades. Therefore, the model evaluation of long-term changes of Hg concentration and deposition levels highly depends on availability of reliable data on historical Hg emissions.

Despite increases in global anthropogenic emissions over the past several decades (*Streets et al.,* 2011), Arctic atmospheric Hg levels have decreased or remained constant (*Cole and Steffen*, 2010; *Cole et al*., 2013, *Berg et al*. 2013). Implications of climate change related factors such as rise in air temperatures (particularly in spring) and reduced sea ice extent and thickness to the Hg levels in the

Arctic ecosystems are complex and multidirectional (*Stern et al.,* 2012; *Bekryaev et al*., 2010; *Cavalieri et al*., 2012).

Fisher et al. (2013) investigated the factors controlling Hg(0) trends in the Arctic from 1979-2008 using global historical anthropogenic emissions inventory of *Streets et al.* (2011) using GEOS-Chem. The model simulated a small increasing trend in Hg(0) concentrations over 30 years mainly reflecting the growth in emissions. Besides, the authors suggested that climate warming may lead to decreased fluxes of Hg from the atmosphere to the cryosphere and increased Hg(0) concentrations in the Arctic. *Chen et al*. (2015) extended the study by *Fisher et al*. (2013) to quantitatively determine the contributions of changes in environmental variables and anthropogenic emissions to Hg trends in the Arctic using anthropogenic emission inventories from AMAP/UNEP for the years 2000, 2005, and 2010. In addition to confirming the results by *Fisher et al*. (2013) in spring and summer, the study found that decrease in Atlantic ocean evasion of Hg at lower latitudes contributed to the decrease in Hg(0) concentrations in the Arctic from November–March.

Dastoor et al. (2015) assessed the impact of changing anthropogenic emissions and meteorology on Hg(0) concentrations and deposition in the Canadian Arctic from 1990-2005 using GEM-MACH-Hg and AMAP anthropogenic emissions (*AMAP*, 2011). Changes in meteorology and anthropogenic emissions were found to contribute equally to the decrease in surface air Hg(0) concentrations in the Canadian Arctic with an overall decline of ~12% from 1990-2005 in agreement with measurements at Alert (*Cole and Steffen*, 2010; *Cole et al.,* 2013). In contrast, the model simulated 15% increase and 5% decrease in net deposition in the High Arctic due to changes in meteorology and decline in emissions in North America and Europe, respectively, resulting in an overall increase of 10% in Hg deposition over a period of 1990-2005. Although the link between Hg deposition and lake sediment fluxes is not fully understood, an increase in deposition of Hg in the Arctic appears to be consistent with observed increases in Hg fluxes in some Arctic lake sediments in recent decades (*Goodsite et al*., 2013).

Despite modelling differences, all studies suggested a dominant role of climate warming related changes in environmental factors on Hg trends in the Arctic. Current Hg models lack a complete representation of the complexity of climate sensitive Hg processes. Fully interactive atmosphere-land-ocean biogeochemical Hg models including detailed representation of sea-ice dynamics are required to close the gap in modelling results.

Future changes of Hg atmospheric concentration and deposition to the ground as a result of changes in anthropogenic emissions, land use and land cover as well as climate change were also investigated

in a number of modelling studies. *Pacyna et al.* (2016) used two chemical transport models (GLEMOS and ECHMERIT) to evaluate future changes of Hg depositions in various geographical regions for three anthropogenic emissions scenarios of 2035 (Fig. 1). The "Current Policy" scenario (CP 2035) predicted a considerable decrease (20-30%) of Hg deposition in Europe and North America and strong (up to 50 %) increase in South and East Asia. According to the "New Policy" scenario (NP 2035) a moderate decrease in Hg deposition (20-30%) was predicted in all regions except for South Asia. Model predictions based on the "Maximum Feasible Reduction" scenario (MFR 2035) demonstrated consistent Hg deposition reduction on a global scale. It should be noted that the geogenic and legacy sources were assumed to be unchanged in this study.

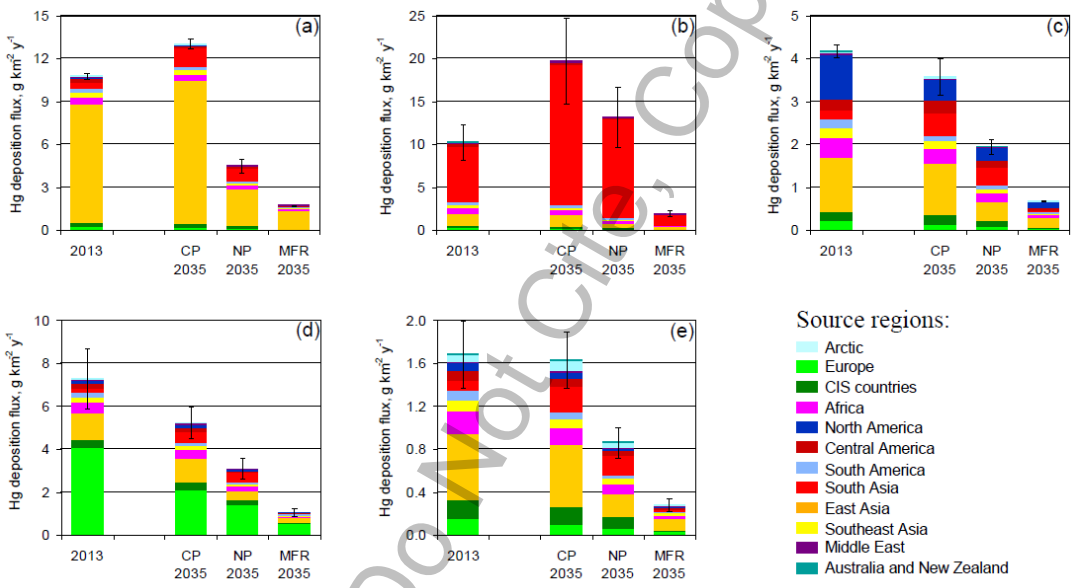

Figure 1. *Source apportionment of Hg deposition from direct anthropogenic sources (average of two models) in 2013 and 2035 in various geographical regions: (a) East Asia, (b) South America, (c) North America, (d) Europe, (e), and the Arctic. Whiskers show deviation between the models. Contribution of natural and secondary emissions are not shown. Source: Pacyna et al. (2016).*

A combined effect of emissions changes and temperature increase associated with climate change was studied by *Lei et al.* (2014) with the CAM-Chem model using three emissions scenarios of 2050 (B1, A1B, A1FI) based on projections developed by the Intergovernmental Panel on Climate Change (IPCC). It was found that all three scenarios predict general increase of total gaseous Hg concentration around the globe due to increasing use in fossil fuel energy. The increase in temperature enhances emissions from land and ocean and accelerates oxidation of Hg^0 leading to increased deposition. The effect of climate change as well as alteration of land cover/land use on

future Hg levels were studied more thoroughly by *Zhang et al.* (2016) by combining a chemical transport model (GEOS-Chem), a general circulation model (GISS GCM 3), and a dynamic vegetation model (LPJ). Using the IPCC A1B scenario for the simulation of 2000-2050 climate change they found that the surface Hg^0 concentration is to increase globally with significant changes occurring over most continental and ocean regions due to changes in atmospheric Hg redox chemistry. Changes in natural vegetation and anthropogenic land use lead to general increases in Hg^0 dry deposition. The gross Hg deposition flux will increase over most continental regions driven by combined changes in climate and land use/land cover. However, these results do not take into account the possible feedback of the deep ocean and terrestrial reservoirs to the future emissions and climate changes.

Amos et al. (2013) used a fully coupled biogeochemical model and showed that even if anthropogenic emissions stay unchangeable, Hg deposition will continue to increase due to effect of the legacy of anthropogenic production emissions accumulated in the ocean. Generally, the atmosphere responds quickly to the termination of future emissions, but long-term changes are sensitive to a number of factors, including historical changes in anthropogenic emissions, air-sea exchange, and Hg burial in deep ocean and coastal sediments (*Amos et al.*, 2014, 2015).

4.5. Region-specific modelling studies

4.5.1. Polar regions

Since GMA 2013, three global Hg models have been applied to study Hg cycling in polar regions - GLEMOS (*Travnikov and Ilyin*, 2009), GEOS-Chem (*Fisher et al*. 2012; *Holmes et al*., 2010), and GEM-MACH-Hg (formerly GRAHM; *Dastoor et al*., 2008; *Durnford et al*., 2012; *Kos et al*., 2013). The largest differences among models in the polar-regions are related with the representation of Hg(0)-Br oxidation rates, Br concentrations, parameterization of photo-reduction and re-emission of Hg(0) from the snowpack, and Hg evasion fluxes from the Arctic Ocean (*Angot et al.,* 2016). *Durnford et al*. (2012) developed and implemented a dynamic multi-layer snowpack-meltwater parameterization in GEM-MACH-Hg. *Fisher et al.* (2012) and *Durnford et al*. (2012) introduced enhanced evasion of Hg from the Arctic Ocean during summer to explain the observed summertime maximum in Hg(0) concentrations (*Steffen et al*. 2005; *Berg et al.* 2013). *Dastoor and Durnford* (2014) found that the summertime concentrations in the Arctic are characterized by two distinct summertime maxima with the peaks varying in time with location and the year. Using GEM-MACH-Hg, the authors demonstrated that early summer peak in Hg(0) concentrations is supported primarily by re-emission of Hg from melting snowpack and meltwater and the late summer peak is supported by evasion of Hg(0) from the Arctic Ocean. *Toyota et al*. (2014) developed a detailed one-dimensional air–snowpack model for interactions of bromine, ozone, and Hg in the springtime Arctic which provided

a physicochemical mechanism for AMDEs and concurrently occurring ozone depletion events (ODEs). The authors also developed a temperature dependent GOM-PBM partitioning mechanism explaining its observed seasonal transition (*Steffen et al*., 2014) and demonstrated that PBM is mainly produced as $HgBr_4^{2-}$ through uptake of GOM into bromine-enriched aerosols after ozone is significantly depleted in the Arctic air masses.

Dastoor and Durnford (2014) conducted a comprehensive evaluation of GEM-MACH-Hg simulated concentrations of Hg(0) and Hg(II) in air, total Hg (THg) concentrations in precipitation and seasonal snowpack, and snow/air Hg fluxes with measurements from 2005-2009 at 4 Arctic sires – Alert, Ny-Ålesund, Amderma, and Barrow (see Fig. 2 for the sites location). The model median concentrations of Hg(0) and Hg(II) were found within the range of observed medians at all locations. Hg concentrations in snow collected during springtime (AMDEs season) are significantly higher at Barrow than at Alert, which was well simulated by the model. Modelled Hg concentrations in seasonal snowpack were also within the measured range.

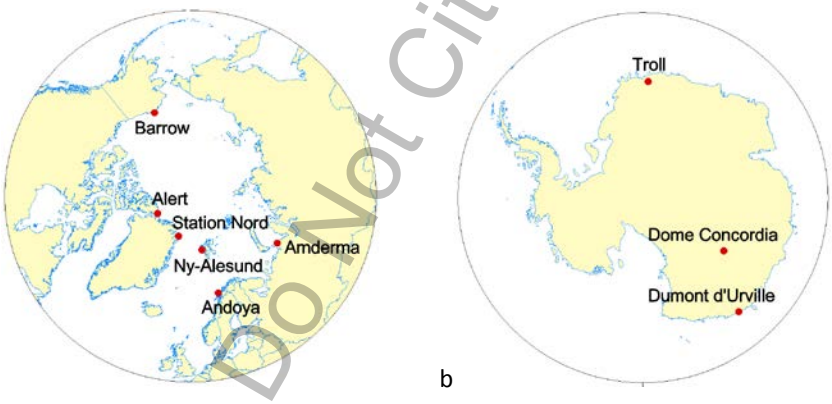

Figure 2: *Location of Arctic (a) and Antarctic (b) ground-based sites used for model evaluation.*

Angot et al. (2016) evaluated GEM-MACH-Hg, GEOS-Chem and GLEMOS using atmospheric monitoring data of Hg concentrations for 2013 at 4 Arctic sites (Alert, Station Nord, Ny-Ålesund and Andøya) and 3 Antarctic sites (Troll, Dome Concordia, and Dumont d'Urville) shown in Fig. 2. In addition, interannual variability in Hg(0) concentrations were evaluated using GEOS-Chem and GEM-MACH-Hg simulations from 2011-2014. The models captured the broad spatial and seasonal patterns in Hg(0) concentrations observed in the Arctic. The decline in Hg(0) concentrations from Andøya, the site closest to European industrialized areas, to Alert, the most northerly site, was well reproduced by the models and suggests transport of anthropogenic Hg from lower latitudes to the Arctic. A more

pronounced seasonal cycle observed at Alert and Station Nord than Ny-Ålesund and Andøya was also captured by the models (Fig. 3).

All models reproduced the characteristic low Hg(0) concentrations in spring and high Hg(0) concentrations in summer. Consistent with observations, the models simulated enhanced total oxidized Hg concentrations (i.e., oxidized gaseous and particulate Hg) at Alert and Ny-Ålesund during the AMDEs season but underestimated the values compared to measurements. At Ny-Ålesund all the models overestimated wet deposition along with overestimation of precipitation amount. The model-measurement discrepancy was attributed to lower collection efficiency of precipitation in polar regions due to frequent strong winds and blowing snow conditions (*Lynch et al*., 2003 and *Prestbo and Gay*, 2009) and to the uncertainties in gas-particle partitioning of oxidized Hg in the models.

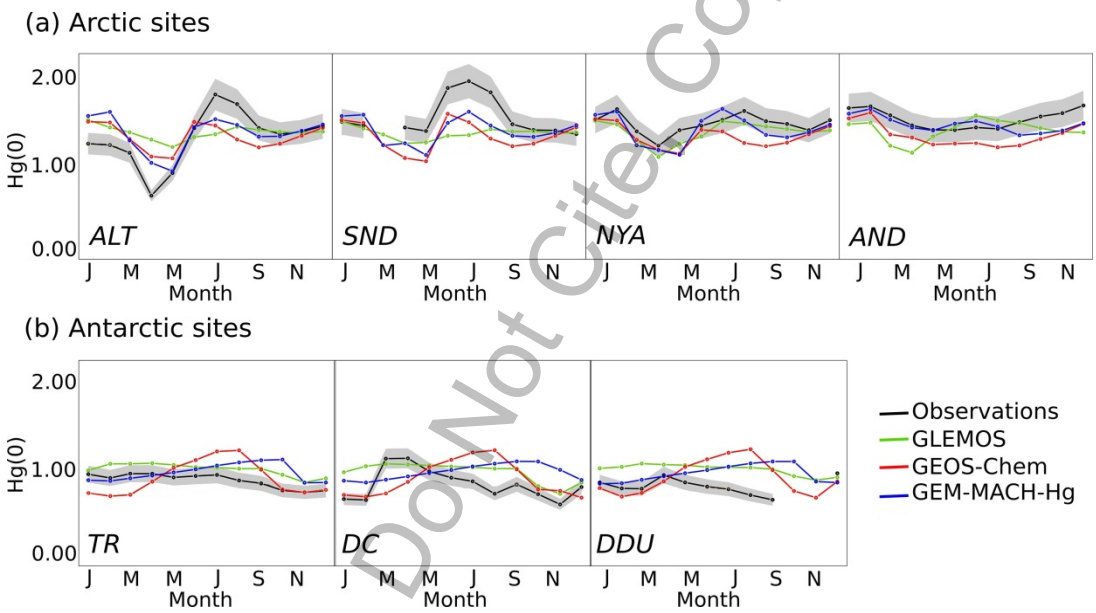

Figure 3: *Year 2013 monthly-averaged Hg(0) concentrations (in ng m^{-3}) at (a) Arctic and (b) Antarctic ground-based sites: observations (in black) and concentrations according to the three global models (GLEMOS in green, GEOS-Chem in blue, GEM-MACH-Hg in red). The grey shaded regions indicate a 10% uncertainty for observations. Adapted from Angot et al. (2016). Only models that explicitly implement high-latitude specific processes are shown.*

Simulated Hg(0) interannual variability in GEOS-Chem and GEM-MACH-Hg in winter was lower than measured which suggests an impact of interannual variability in anthropogenic emissions; the models used 2010 global anthropogenic Hg emissions (*AMAP/UNEP*, 2010) for simulations from 2011-2014. Interannual variability in the frequency of AMDEs was fairly well reproduced by GEM-

MACH-Hg but not by GEOS-Chem. Real-time modelling of the distribution of bromine concentrations and sea-ice dynamics is needed to improve the models (*Moore et al*., 2014).

In contrast, at Antarctic sites, the models overestimated Hg(0) concentrations and failed to reproduce observed seasonal patterns in Hg(0) concentrations (Fig. 3). GEM-MACH-Hg and GEOS-Chem simulated increasing Hg(0) concentrations at all sites over the course of winter in contradiction with observations; whereas, GLEMOS simulated lower than observed wintertime decline in Hg(0) concentrations at Dumont d'Urville and Dome Concordia (*Angot et al*., 2016). High summertime variability and strong diurnal cycle in Hg(0) concentrations observed at Dumont d'Urville and Dome Concordia were also not well reproduced by the models. GEM-MACH-Hg did not simulate the infrequent AMDEs observed at Troll and Dumont d'Urville in spring; whereas, GEOS-Chem simulated AMDEs at DDU with somewhat higher frequency than observed. *Angot et al*. (2016) attributed poor model simulation of Hg at the Antarctic sites to missing local Hg(0) oxidation pathways involving OH, O_3, NOx, and RO_2 radicals and air circulation, and bias in southern hemispheric emissions including oceanic evasion in the models.

Modelling estimates of Hg mass fluxes in the Arctic including the Arctic Ocean were provided by *Fisher et al.* (2012), *Durnford et al.* (2012) and *Dastoor and Durnford* (2014). Using GEOS-Chem, *Fisher et al.* (2012) estimated Hg deposition of 55 Mg y^{-1} (i.e., 25 Mg y^{-1} directly to open ocean, 20 Mg y^{-1} to ocean via snow melt on sea ice, and 10 Mg y^{-1} to land via snow melt), evasion from ocean of 90 Mg y^{-1} and a net surface loss of 35 Mg y^{-1} in the Arctic north of 70°. In contrast, using GEM-MACH-Hg, *Durnford et al*. (2012) estimated Hg deposition of 153 Mg y^{-1} (i.e., 58 Mg y^{-1} directly to open ocean, 50 Mg y^{-1} to ocean via snow melt on sea ice, 29 Mg y^{-1} directly to land, and 16 Mg y^{-1} to land via snow melt), emission of 36 Mg y^{-1} (i.e., 33 Mg y^{-1} from ocean and 3 Mg y^{-1} from land) and a net surface gain of 117 Mg y^{-1} in the Arctic north of 66.5°. Thus, *Fisher et al.* (2012) concluded that Arctic Ocean is a net source of Hg to the atmosphere, i.e., 45 Mg y^{-1}; whereas, *Durnford et al*. (2012) concluded that Arctic Ocean is a sink of atmospheric Hg, i.e., 75 Mg y^{-1}. In comparison, GLEMOS estimated the yearly net gain of Hg in the Arctic to be 131 Mg y^{-1} (*Travnikov and Ilyin*, 2009).

Model disagreements in the estimates of atmosphere-ocean-snowpack Hg fluxes indicate sources of uncertainties in the models. Constraining models in the polar regions is challenging due to insufficient measurements (*Dastoor and Durnford*, 2014; *Angot et al*., 2016). *Fisher et al*. (2012) inferred that 95 Mg y^{-1} input of Hg from circumpolar rivers (and coastal erosion) resulting in 90 Mg y^{-1} evasion of Hg from the Arctic Ocean was required to balance the observed summertime peak in Hg(0) concentrations at the Arctic sites. In contrast, *Durnford et al*. (2012) found that 33 Mg y^{-1} Hg evasion from the Arctic Ocean was sufficient to reproduce the summertime peak Hg(0)

concentrations in the Arctic. *Dastoor and Durnford* (2014) estimated riverine Hg export to the Arctic Ocean from North American, Russian and all Arctic watersheds in the range of 2.8-5.6, 12.7-25.4 and 15.5-31.0 Mg y^{-1}, respectively, based on GEM-MACH-Hg simulated Hg in meltwater. Using MITgcm ocean model and GEOS-Chem, *Zhang et al*. (2015) concluded that an input of 63 Mg y^{-1} of Hg discharge from rivers and coastal erosion to the Arctic Ocean was needed to reproduce the observed summer maximum in atmospheric Hg(0) concentrations. Riverine discharge to the Arctic Ocean is poorly constrained by observations with estimates ranging from 12.5 to 44 Mg y^{-1} (*Outridge et al*., 2008; *Amos et al*., 2014). *Zhang et al*. (2015) noted that enhanced turbulence associated with sea ice dynamics facilitates increased evasion of Hg discharged by Arctic rivers in estuaries resulting in a much larger portion of riverine Hg in the Arctic Ocean subjected to evasion than estimated in *Fisher et al*. (2012). In addition, *Fisher et al*. (2012) assumed that the Hg input from rivers is uniformly distributed in the entire Arctic Ocean; whereas, latitudinal variation in Hg evasion from the Arctic Ocean was considered in *Durnford et al*. (2012) and *Zhang et al*. (2015) which is supported by observations (*Andersson et al*., 2008; *Hirdman et al*. 2009; *Sommar et al*, 2010). Other sources of differences in models were related with the parameterizations of bromine concentrations and Hg snowpack/meltwater processes (*Dastoor and Durnford*, 2014).

4.5.2. Europe

In recent years, the development of regional atmospheric Hg models for Europe was supported by the FP7 project GMOS (Global Mercury Observations System). Mercury chemistry was implemented into the on-line coupled meteorological CTM WRF-Chem by *Gencarelli et al.* (2014) and the CCLM-CMAQ model was further developed (*Bieser et al.,* 2014; *Zhu et al.,* 2015). These models have been used to evaluate key processes and identify their impact on Hg dispersion and deposition in Europe (*Gencarelli et al*., 2016; *Bieser et al*., 2017).

As it follows from recent estimates by *Muntean et al*. (2014) Hg emissions in Europe continue to decrease, but with different rates for each Hg species. Due to technological development, emissions of GOM are declining faster than total Hg emissions, which affects the regional deposition and global transport patterns. This finding was further confirmed by model studies were the models tendency to overestimate ground based GOM concentrations could be attributed to the speciation of primary anthropogenic Hg emissions (*Bieser et al*., 2014; 2017). Moreover, airborne in situ measurements at a modern coal fired power plant did not detect any GOM 1 km downwind from the stack (*Weigelt et al.,* 2016).

The models have in common, that the modelled annual wet deposition fluxes are in good agreement with observations. This was found for regional (*Gencarelli et al*., 2014; *Bieser et al.,* 2014) and global

models (*Muntean et al*., 2014). At the same time, models tend to underestimate TGM concentrations for Europe. A behaviour which is also seen in the results from global models (*Muntean et al.*, 2014; *Chen et al*., 2013). The reason for this is not understood yet. In a global long term simulation with the GEOS-Chem model *Muntean et al*. (2014) showed that modelled TGM concentrations were closer to observations in the 1990s but that the model overestimates the decreasing tend over the last decades. Thus, the emission inventories might play a role for this. This is also in line, with the fact that new regional emission models lead to higher estimates for European Hg emissions (*Rafaj et al*., 2014).

Moreover, a recent study with a newly developed regional multi-media model indicates that an underestimation of the air-sea exchange from regional oceans could be a source for the model bias in Europe (*Bieser and Schrum*, 2016). Figure 4 depicts the impact of air-sea exchange on Hg concentrations at two ground based stations in Europe. It can be seen, that close to the ocean (Zingst) air-sea exchange has a large impact on GEM concentrations. This effect, albeit less pronounced, was also observed at a station 200 km inland (Waldhof).

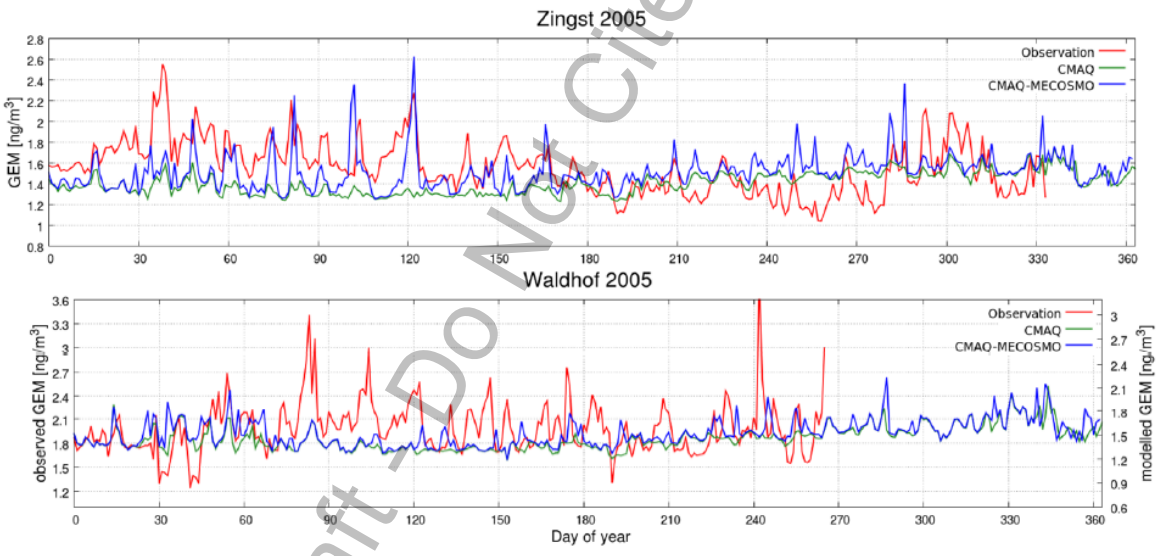

Figure 4: *Impact of air-sea exchange on atmospheric Hg concentrations at two ground based observations sites in Germany: observation (red), atmospheric model (green), coupled ocean-atmospheric model (blue) (Bieser and Schrum, 2016).*

A first model analysis on the vertical distribution of Hg in Europe was recently published (*Bieser et al.*, 2017). Based on aircraft based observations, it was found that models are generally able to reproduce the GEM gradient from the surface up to the tropopause (Fig. 4). Moreover, models were able to reproduce the GOM gradient inside the planetary boundary layer, in those cases where a low

GOM fraction in the anthropogenic emissions was assumed. This is in line with the findings on decreasing GOM fraction in European Hg emissions discussed earlier.

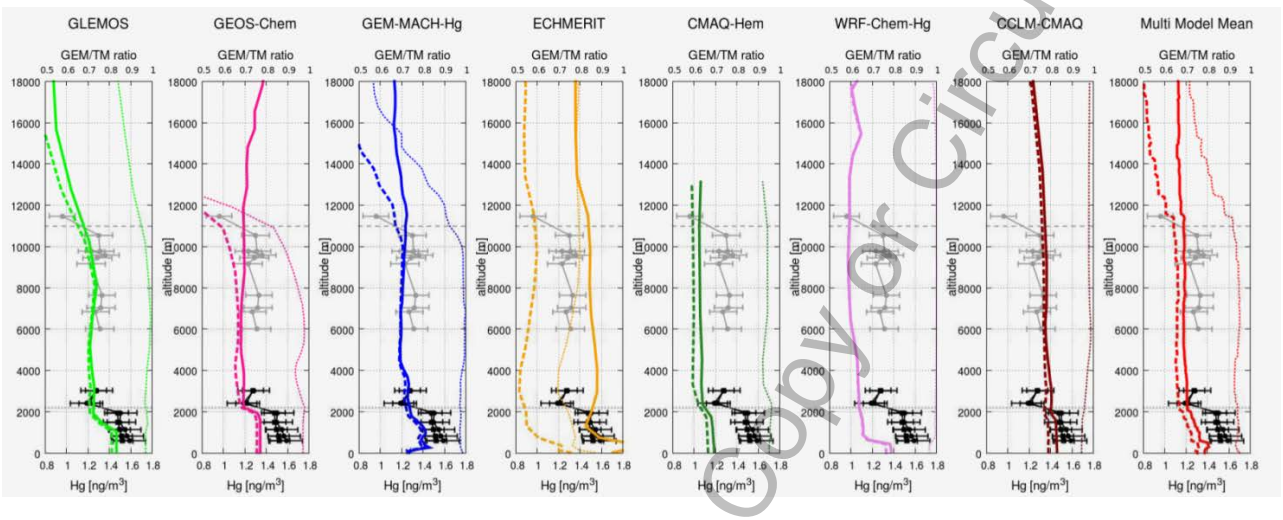

Figure 4: *Vertical profiles at Leipzig, Germany 23rd August 2013 from two aircraft campaigns and simulations with seven atmospheric chemistry transport models. Black dots are observations from the European Tropospheric Mercury Experiment (ETMEP), grey dots are observations from the CARIBIC civil passenger aircraft. The coloured lines indicate modelled TM (solid) and GEM (dashed) concentrations. The dotted lines depict the GEM/TM ratio. Source: Bieser et al. (2017).*

The impact of long range transport on European Hg deposition has been addressed before (*UNEP*, 2015). Since then, there has been a new study on the global transport of Hg from Asia (*Chen et al.,* 2015). Here, the estimated contribution of Chinese emissions to Hg deposition in Europe is only 3.5%, which is much smaller than previous estimates of 20% (*UNEP,* 2015). The impact of long range transport on regional Hg deposition in Europe is strongly dependent on the lifetime of Hg in the atmospheric models. A new study by *Horowitz et al*. (2017) indicates that organic aerosols mediate photolytic reduction of oxidized Hg species in the aqueous phase leading to an increased life time of Hg in the atmosphere. Due to the high concentration of organic aerosols in China current models might underestimate the long range transport due to an overestimation of atmospheric oxidation. *De Simone et al*. (2015, 2016) investigated the impact of biomass burning on atmospheric Hg concentrations and deposition. Especially wild fires in the boreal forests can have a large impact on regional Hg concentration and deposition. For Europe, they estimate the fraction of Hg deposition due to biomass burning between 5% and 10%.

4.5.3. North America

CMAQ, with global boundary conditions estimated with the MOZART model, was used to estimate atmospheric Hg deposition to the Great Lakes for 2005 (*Grant et al.*, 2014). U.S. emissions from power plants had the largest impact on Lake Erie. The model tended to overestimate wet deposition in the Great Lakes region. In another CMAQ-based investigation, the model was used with boundary conditions from GEOS-Chem, and alternatively, GRAHM, to estimate atmospheric Hg deposition in the United States (*Myers et al*., 2013) in a series of 2001-2005 case studies. Simulation results were significantly influenced by the choice of boundary conditions. CMAQ, with a new aqueous-phase oxidized Hg reduction chemical mechanism (involving dicarboxylic acids) and GEOS-Chem boundary conditions, was used to simulate Hg fate and transport in the U.S. during 2001-2002. Results for wet deposition with the new chemical mechanism were found to be more consistent with observations than earlier mechanisms used in CMAQ. Using a weight-of-evidence approach, *Sunderland et al*. (2016) argued that historical EPA CMAQ-based modelling may have underestimated the impact of local and regional sources on near-field Hg deposition in the U.S., and consequently underestimated the benefits of Hg emissions reductions.

The GEOS-Chem model was used to estimate the cumulative benefits of domestic and international Hg controls for atmospheric deposition – and subsequent public health impacts – in the U.S. through 2050 (*Giang and Selin*, 2016). For the same amount of avoided Hg emissions, domestic reductions were estimated to have nearly an order of magnitude higher public health benefit than international actions. The CAM-Chem-Hg model was used to estimate present day (ca. 2000) (*Lei et al*., 2013) and future (ca. 2050) (*Lei et al*., 2014) atmospheric Hg concentrations and deposition in the U.S., as influenced by different scenarios of changes in U.S. and global emissions, and different climate change scenarios. Concentrations and deposition in the U.S. increased significantly in scenarios with higher future emissions and higher atmospheric temperatures. Under the most impacted scenario considered, climate change alone caused an approximate 50-100% increase in atmospheric Hg concentrations in the U.S. When increased Hg emissions in this scenario were included, the average Hg(0), GOM, and PBM concentrations in the U.S. increased by a factors of ~2.5x, ~5x, and ~3x, respectively. The GRE-CAPS model – which included a version of the regional CAMx model - was used to investigate the influence of climate change on atmospheric Hg deposition in the Eastern U.S. (*Megaritis et al.*, 2014). Simulations for the present day (ca. 2000's) were compared with climate-change-influenced simulations for the year 2050, assuming constant 2001 Hg emissions. The study found that average deposition in the U.S. increased by about ~5% due to climate-change impacts (e.g., enhanced atmospheric oxidation of GEM at higher temperatures), but regional differences were found (e.g., related to changes in precipitation patterns).

The HYSPLIT-Hg model was used to estimate 2005 atmospheric Hg deposition to the Great Lakes (*Cohen et al.*, 2016). Results for a base case and 10 alternative model configurations were developed, examining the sensitivity of the results to different assumptions regarding atmospheric reaction rates and chemical mechanisms. Model evaluation against measurements in the Great Lakes region showed good agreement between modelled and measured wet deposition and Hg(0) concentrations, but the model tended to overpredict reported GOM and PBM concentrations. The total deposition and source-attribution for that deposition was similar to that found by *Grant et al.* (2014) (e.g., see Figure 5). Lake Erie, downwind of significant local/regional emissions sources, was estimated by the model to be the most impacted by direct anthropogenic emissions (58% of the base case total deposition), while Lake Superior, with the fewest upwind local/regional sources, was the least impacted (27%). The U.S. was the largest national contributor, followed by China, contributing 25% and 6%, respectively, on average, for the Great Lakes. The contribution of U.S. direct anthropogenic emissions to total Hg deposition varied between 46% for the base case (with a range of 24–51% over all model configurations) for Lake Erie and 11% (range 6–13%) for Lake Superior. The relative contributions of different sources are illustrated in Figure 6 for the base case simulation. These results were used in an International Joint Commission report (*IJC*, 2015) which called for increased monitoring and modelling of atmospheric Hg in the Great Lakes region.

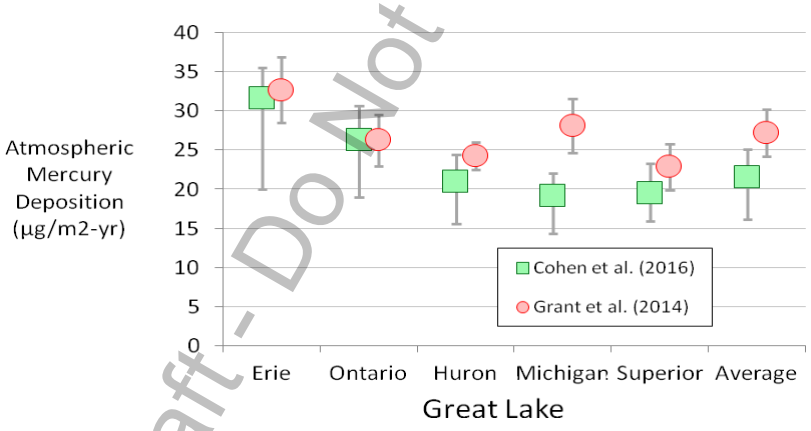

Figure 5. *Atmospheric Hg deposition flux to the Great Lakes for 2005, estimated by CMAQ (Grant et al., 2014) and HYSPLIT-Hg (Cohen et al., 2016). CMAQ error bars shown are the reported range in estimates for each lake. HYSPLIT-Hg error bars shown are the range found in the 10 alternate model configurations used in the analysis. The Great Lakes summary values shown are based on an area-weighted average of individual-lake results.*

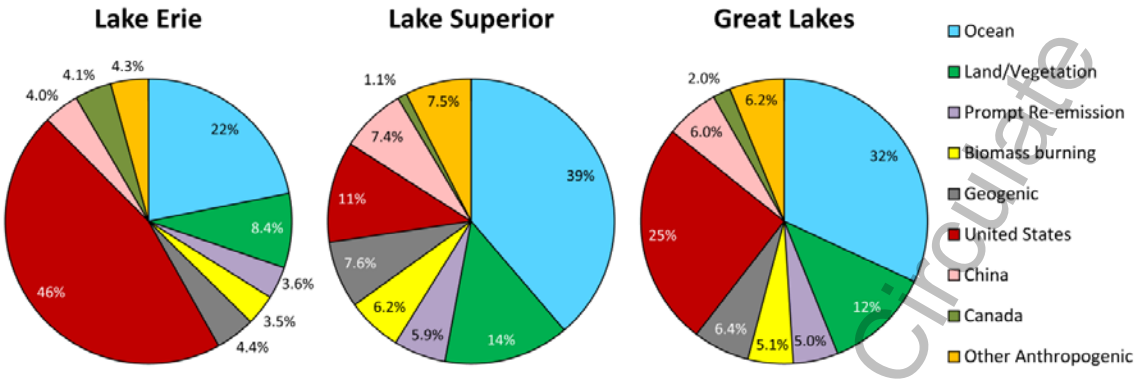

8703

8704 ***Figure 6.*** *Relative contributions of different source categories to 2005 atmospheric Hg deposition to*
8705 *Lake Erie, Lake Superior, and an area-weighted average for the Great Lakes, estimated by the*
8706 *HYSPLIT-Hg model (Cohen et al., 2016) (base-case simulation). The values shown for specific*
8707 *countries (United States, China, and Canada) and for all other countries ("Other Anthropogenic")*
8708 *include only the contributions from direct, anthropogenic emissions and do not include contributions*
8709 *arising from re-emissions of previously deposited material from terrestrial or oceanic surfaces.*

8710 A number of analyses were conducted in which measurements of atmospheric concentrations were
8711 combined with back-trajectory and other receptor-based modelling approaches to assess the relative
8712 importance of different source regions and other factors to the atmospheric Hg arriving at the
8713 measurement site (see Table 1 for references). In most cases, the HYSPLIT model (*Stein et al.,* 2015)
8714 was used for simulating back-trajectories. Similar studies were carried out for flight-based
8715 measurements of atmosphere Hg concentrations above the surface, utilizing back-trajectories and/or
8716 other model simulations, above Tullahoma, TN (*Brooks et al*., 2014), Texas and the Southeastern U.S.
8717 (*Ambrose et al.,* 2015; *Gratz et al*., 2015; *Shah et al*., 2016), and Lake Michigan (*Gratz et al*., 2016).

8718 **Table 1.** Measurement sites analysed with receptor-based modelling

Measurement site	Country	Back-trajectory Study
Beltsville, MD	USA	*Ren et al*., 2016
Celestun, Yucatan	MEX	*Velasco et al*., 2016
Chicago, IL	USA	*Gratz et al*., 2013a
Dartmouth, NS	CAN	*Cheng et al*., 2013a; *Cheng et al*., 2016
Grand Bay, MS	USA	*Ren et al.,* 2014; *Rolison et al*., 2013
Holland MI	USA	*Gratz et al*., 2013a
Huntington Forest, NY	USA	*Zhou et al*., 2017; *Choi et al*., 2013; *Cheng et al*., 2013b
Illinois (several sites)	USA	*Gratz et al*., 2013b; *Lynam et al*., 2014
Kejimkujik, NS	CAN	*Cheng et al*., 2013a; *Cheng et al*., 2016
Oxford, MS	USA	*Jiang et al*., 2013
Pensacola, FL	USA	*Huang et al*., 2016; *Demers et al*., 2015
Piney Reservoir, MD	USA	*Castro and Sherwell,* 2015
Reno, NV	USA	*Gustin et al*., 2016

Rochester, NY	USA	*Choi et al.*, 2013
Steubenville, OH	USA	*White et al*., 2013
Underhill, VT	USA	*Zhou et al.*, 2017
Western U.S. (several sites)	USA	*Wright et al*., 2014; *Huang and Gustin*, 2015; *Gustin et al*., 2016
Windsor, ON	CAN	*Xu et al.,* 2014

In a hybrid analysis combining fate-and-transport modelling with measurements, GEOS-Chem was used to examine trends in Hg wet deposition over the United States over the 2004-2010 period (*Zhang and Jaegle*, 2013). The modelling results were subtracted from the observations to assess the roles of changing meteorology and emissions on observed wet deposition at 47 U.S. sites. In the Northeast and Midwest U.S., approximately half of the decreasing trend in Hg concentrations in precipitation could be explained by decreasing U.S. emissions over the study period.

4.5.4. East Asia

East Asia (including Southeast Asia) is the largest source region of atmospheric Hg release worldwide, with China as the largest emitter. According to *GMA 2013*, Hg release in East and Southeast Asia accounts for 40% of global anthropogenic emission in 2010. Mercury outflow from East Asia has been regarded as a concern to global Hg pollution (*Jaffe et al*., 2005; *Lin et al*., 2010; *Chen et al*., 2014).

The rapid economic growth and improving air emission control in East Asia change the anthropogenic Hg emission and speciation readily within a relatively short period of time. As better emission data become available, reassessment using updated emission data is necessary. For example, *Wu et al*. (2016) applied updated industrial activity statistics and emission factors to estimate anthropogenic Hg release in China from 1978 to 2014, and found that the emission varied significantly over time due to increased industrial production, energy use and implementation of emission control measures. Atmospheric Hg emission in China peaked in 2011 at 565 Mg y^{-1} and then dropped to 531 Mg y^{-1} in 2014. More importantly, the emission speciation gradually shifted to a larger fraction of oxidized Hg (56/43/3 for Hg0/HgII/Hgp in 2014). Such an emission speciation shift indicates increased local deposition and reduced emission outflow.

Wang et al. (2016b) re-evaluated the natural release of elemental Hg vapour from soil, vegetation and water surfaces using new soil Hg data in China and updated model schemes with physicochemical parameters reported recently. They found a distinct spatial distribution of estimated Hg release compared to the data reported by *Shetty et al*. (2008), despite a similar net natural release at ~460 Mg y^{-1} in China. Such a spatial distribution transition also has an impact on regional model results.

A number of regional and global scale modelling studies simulated atmospheric Hg levels in China and the East Asia region (e.g. *Lin et al*., 2010; *Pan et al*., 2010; *Chen et al*., 2014; *Chen et al*., 2015; *Zhu et al*., 2015; *Wang et al*., 2016a). It should be noted that most model results are not directly comparable due to differences in the emission inventory (particularly, natural emissions since many earlier studies did not specify the quantity and spatial distribution), Hg chemistry and model configuration. In general, regional models reproduced Hg concentrations more representative of the observed elevated levels in urban and industrial areas. Most global model results appear to be relatively consistent, estimating that Asian emissions contribute to 16-25% of Hg deposition in North America and 10-15% in the European region, except for one study (*Chen et al.,* 2014) reporting <5% of contribution in both regions.

The results of two regional modelling studies using CMAQ-Hg with identical model specifications are directly comparable (*Lin et al*., 2010; *Wang et al.* 2016a). The two modelling assessments use the same model configuration of CMAQ-Hg with different emission inventories: from (*Street et al.,* 2005; *Shetty et al*., 2008) in the former, and from (*Wu et al.,* 2016; *Wang et al*., 2016b) in the latter. The difference in the annual budgets is mainly caused by the reduced anthropogenic emission in the region, increased fraction of HgII, and a change in the spatial distribution of natural emission. Given the changes in emissions, the transport budget from East Asia by *Wang et al.* (2016a) is 25% lower than the earlier estimate by *Lin et al.* (2010), as shown in Figure 7. In addition, the greater Hg mass accumulated within the regional domain in *Wang et al.* (2016a) also better explain the elevated atmospheric Hg concentrations in China. More modelling studies are still needed in this region. Recent observational data obtained from the ambient monitoring network in China (*Fu et al.,* 2015) provide a unique opportunity to better understand the chemical transport of atmospheric in a region undergoing dynamic emission changes.

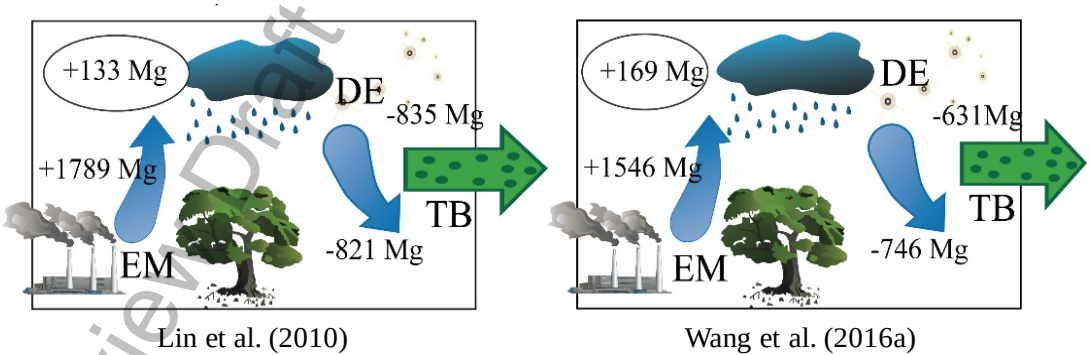

Lin et al. (2010) Wang et al. (2016a)

Figure 7: *Comparison of annual Hg mass budget in East Asia by Lin et al. (2010) and Wang et al. (2016a). EM is emission; DE is deposition; TB is transport budget.*

4.6. Conclusions

A number of regional and global models have been used to simulate the atmospheric fate and transport of Hg, using meteorological data and emissions inventories as inputs and atmospheric measurements to evaluate the results. Significant uncertainties remain in model physics (e.g., gas-particle partitioning and deposition processes) and chemistry (e.g., elemental Hg oxidation mechanisms), as well as in model inputs (e.g., emissions amounts and speciation) and measurements used for evaluation. Nevertheless, the scientific understanding of atmospheric Hg as represented in the models has progressed to the point where useful policy-relevant information about source-receptor relationships can be derived. This also implies that models can be used to provide first estimates of the effects on Hg-deposition of emission reductions, both regionally and globally. As improvements are made in understanding and model-related data, uncertainties in model results will be lessened and will become even more useful.

Atmospheric measurements are essential to evaluate and improve models; given the uncertainties noted above, models must continually be tested by comparison against measurements. At the same time, measurements alone cannot provide the depth of source-receptor and trend explanation information that can be obtained by models. Likewise, uncertainties in emissions inventories have emerged as a critical limitation in atmospheric model analyses, and the improvement of these fundamental model inputs is essential to improve model accuracy.

(To be updated based on new simulation results)

References

Agnan Y., T. Le Dantec, C. W. Moore, G. C. Edwards, and D. Obrist (2016) New Constraints on Terrestrial Surface-Atmosphere Fluxes of Gaseous Elemental Mercury Using a Global Database, *Environmental Science and Technology*, *50*(2), 507–524, doi:10.1021/acs.est.5b04013.

AMAP (2014) Global Anthropogenic Emissions of Mercury to the Atmosphere, www.amap.no/mercury-emissions/datasets.

AMAP (2011) AMAP assessment 2011: mercury in the Arctic. Oslo, Norway: Arctic Monitoring and Assessment Programme (AMAP); (pp. xiv +193).

Ambrose J.L., Gratz L.E., Jaffe D.A., Campos T., Flocke F.M., Knapp D.J., Stechman D.M., Stell M., Weinheimer A. J., Cantrell C.A., and Mauldin R.L. (2015) Mercury Emission Ratios from Coal-Fired Power Plants in the Southeastern United States during NOMADSS, *Environmental Science & Technology*, 49, 10389-10397, 10.1021/acs.est.5b01755.

Amos H.M., Jacob D.J., Streets, D.G. , and Sunderland E.M. (2013) Legacy impacts of all-time anthropogenic emissions on the global mercury cycle, *Global Biogeochemical Cycles* **27**(2), 410--421.

Amos H.M., D.J. Jacob, D. Kocman, H.M. Horowitz, Y. Zhang, S. Dutkiewicz, M. Horvat, E.S. Corbitt, D.P. Krabbenhoft, and E.M. Sunderland (2014) Global biogeochemical implications of mercury discharges from rivers and sediment burial, *Environ. Sci. Technol*., 48(16), 9514–9522.

Amos H.M., Sonke J.E., Obrist D., Robins N., Hagan N., Horowitz H.M., Mason R.P., Witt M., Hedgecock I.M., Corbitt E.S., and Sunderland E.M. (2015) Observational and Modelling Constraints on Global Anthropogenic Enrichment of Mercury, *Environ. Sci. Technol.* 49(7), 4036--4047.

Andersson, M.; Sommar, J.; Gårdfeldt, K.; Lindqvist, O. (2008) Enhanced concentrations of dissolved gaseous mercury in the surface waters of the Arctic Ocean. *Mar. Chem.*, *110* (3-4), 190–194; DOI 10.1016/j.marchem.2008.04.002.

Angot H., Dastoor A., De Simone F., Gårdfeldt K., Gencarelli C.N., Hedgecock I.M., Langer S., Magand O., Mastromonaco M.N., Nordstrøm C., Pfaffhuber K.A., Pirrone N., Ryjkov A., Selin N.E., Skov H., Song S., Sprovieri F., Steffen A., Toyota K., Travnikov O., Yang X., and Dommergue A. (2016) Chemical cycling and deposition of atmospheric mercury in polar regions: review of recent measurements and comparison with models*, Atmos. Chem. Phys*., 16, 10735-10763, doi:10.5194/acp-16-10735-2016.

Ariya P.A., Amyot M., Dastoor A., Deeds D., Feinberg A., Kos G., Poulain A., Ryjkov A., Semeniuk K., Subir M. & Toyota K. (2015) Mercury Physicochemical and Biogeochemical Transformation in the Atmosphere and at Atmospheric Interfaces: A Review and Future Directions, *Chemical Reviews* 115(10), 3760-3802.

Auzmendi-Murua I., Castillo Ál. & Bozzelli J.W. (2014) Mercury Oxidation via Chlorine, Bromine, and Iodine under Atmospheric Conditions: Thermochemistry and Kinetics, *The Journal of Physical Chemistry A* 118(16), 2959-2975.

Bekryaev R.V., Polyakov I.V., Alexeev V.A. (2010) Role of polar amplification in long-term surface air temperature variations and modern arctic warming. *J. Clim.,* 23(14), 3888-3906.

Berg T., Pfaffhuber K.A., Cole A.S., Engelsen O. and Steffen A. (2013) Ten-year trends in atmospheric mercury concentrations, meteorological effects and climate variables at Zeppelin, Ny-Alesund, Atmospheric Chemistry and Physics, 13, 6575-6586.

Bieser, J., Slemr, F., Ambrose, J., Brenninkmeijer, C., Brooks, S., Dastoor, A., DeSimone, F., Ebinghaus, R., Gencarelli, C. N., Geyer, B., Gratz, L. E., Hedgecock, I. M., Jaffe, D., Kelley, P., Lin, C.-J., Jaegle, L., Matthias, V., Ryjkov, A., Selin, N. E., Song, S., Travnikov, O., Weigelt, A., Luke, W., Ren, X., Zahn, A., Yang, X., Zhu, Y., and Pirrone, N. (2017) Multi-model study of mercury dispersion in the atmosphere: vertical and interhemispheric distribution of mercury species, Atmos. Chem. Phys., 17, 6925-6955, https://doi.org/10.5194/acp-17-6925-2017.

Bieser J. and Schrum C. (2016) Impact of marine mercury cycling on coastal atmospheric mercury concentrations in the North- and Baltic Sea region. Elementa 111, doi: 10.12952/journal.elementa.000111.

Bieser J., De Simone F., Gencarelli C.N., Hedgecock I.M., Matthias V., Travnikov O., Weigelt A. (2014) A diagnostic evaluation of modelled mercury wet deposition in Europe using atmospheric speciated high-resolution observations, *Environ. Science and Pollution Research* 21 (16).

Brooks S., Ren X., Cohen M., Luke W.T., Kelley P., Artz R., Hynes A., Landing W., and Martos B. (2014) Airborne Vertical Profiling of Mercury Speciation near Tullahoma, TN, USA, *Atmosphere*, 5, 557-574, 10.3390/atmos5030557.

Castro M.S. and Sherwell J. (2015) Effectiveness of Emission Controls to Reduce the Atmospheric Concentrations of Mercury, *Environmental Science & Technology*, 49, 14000-14007, 10.1021/acs.est.5b03576.

Cavalieri D.J. and Parkinson C.L. (2012) Arctic sea ice variability and trends, 1979-2010. *The Cryosphere*, 6(4): 881-889.

Chen G.Q., J.S. Li, B. Chen, C. Wen, Q. Yang, A. Alsaedi, and T. Hayat (2016) An overview of mercury emissions by global fuel combustion: The impact of international trade, *Renewable and Sustainable Energy Reviews*, *65*, 345–355, doi:10.1016/j.rser.2016.06.049.

Cheng I., Zhang L., and Xu X. (2016) Impact of Measurement Uncertainties on Receptor Modelling of Speciated Atmospheric Mercury, *Scientific Reports*, 6, 10.1038/srep20676.

Chen H.S., Wang Z.F., Li J., Tang X., Ge B.Z., Wu X.L., Wild O., Carmichael G.R. (2015) GNAQPMS-Hg v1.0, a global nested atmospheric mercury transport model: model description, evaluation and application to trans-boundary transport of Chinese anthropogenic emissions. *Geosci. Model Dev*., 8, 2857–2876. doi:10.5194/gmd-8-2857-2015.

Chen L., Y. Zhang, D.J. Jacob, A.L. Soerensen, J.A. Fisher, H.M. Horowitz, E.S. Corbitt, and X. Wang (2015) A decline in Arctic Ocean mercury suggested by differences in decadal trends of atmospheric mercury between the Arctic and northern midlatitudes, *Geophysical Research Letters*, *42*(14), 6076–6083, doi:10.1002/2015GL064051.

Cheng I., X. Xu, and L. Zhang (2015) Overview of receptor-based source apportionment studies for speciated atmospheric mercury, *Atmospheric Chemistry and Physics*, *15*(14), 7877–7895, doi:10.5194/acp-15-7877-2015.

Chen L., H.H. Wang, J.F. Liu, Y.D. Tong, L.B. Ou, W. Zhang, D. Hu, C. Chen, and X. J. Wang (2014) Intercontinental transport and deposition patterns of atmospheric mercury from anthropogenic emissions, *Atmospheric Chemistry and Physics*, *14*(18), 10163–10176, doi:10.5194/acp-14-10163-2014.

Cheng I., Zhang L., Blanchard P., Dalziel J., and Tordon R. (2013a) Concentration-weighted trajectory approach to identifying potential sources of speciated atmospheric mercury at an urban coastal site in Nova Scotia, Canada, *Atmospheric Chemistry and Physics*, 13, 6031-6048, 10.5194/acp-13-6031-2013.

Cheng I., Zhang L., Blanchard P., Dalziel J., Tordon R., Huang J., and Holsen T.M. (2013b) Comparisons of mercury sources and atmospheric mercury processes between a coastal and inland site, *Journal of Geophysical Research-Atmospheres*, 118, 2434-2443, 10.1002/jgrd.50169.

Choi H.-D., Huang J., Mondal S., and Holsen T. M. (2013) Variation in concentrations of three mercury (Hg) forms at a rural and a suburban site in New York State, *Science of the Total Environment*, 448, 96-106, 10.1016/j.scitotenv.2012.08.052, 2013.

Coburn S., B. Dix, E. Edgerton, C. D Holmes, D. Kinnison, Q. Liang, A. Ter Schure, S. Wang, and R. Volkamer (2016) Mercury oxidation from bromine chemistry in the free troposphere over the southeastern US, *Atmospheric Chemistry and Physics*, *16*(6), 3743–3760, doi:10.5194/acp-16-3743-2016.

Cohen M.D., Draxler R.R., Artz R.S., Blanchard P., Gustin M.S., Han Y., Holsen T.A., Jaffe D.A., Kelley P., Lei H., Loughner C.P., Luke W.T., Lyman S.L., Niemi D., Pacyna J.M., Pilote M., Poissant L., Ratte D., Ren X., Steenhuisen F., Steffen A., Tordon R., and Wilson S. (2016) Modelling the global atmospheric transport and deposition of mercury to the Great Lakes, Elementa, 4:000118, 10.12952/journal.elementa.000118.

Cole A.S. and Steffen A. (2010) Trends in long-term gaseous mercury observations in the Arctic and effects of temperature and other atmospheric conditions, *Atmos. Chem. Phys*., 10, 4661-4672, 10.5194/acp-10-4661-2010.

Cole A.S., Steffen A., Pfaffhuber K.A., Berg T., Pilote M., Poissant L., Tordon R., and Hung H. (2013) Ten-year trends of atmospheric mercury in the high Arctic compared to Canadian sub-Arctic and mid-latitudes sites, *Atmospheric Chemistry and Physics*, 13, 1535-1545.

Dastoor A.P. and Durnford D.A. (2014) Arctic ocean: is it a sink or a source of atmospheric mercury?, *Environmental Science and Technology*, 48, 1707-1717.

Dastoor A.P., Davignon D., Theys N., Van Roozendael M., Steffen A., and Ariya P.A. (2008) Modelling dynamic exchange of gaseous elemental mercury at polar sunrise, *Environmental Science and Technology*, 42, 5183-5188.

Dastoor A., Ryzhkov A., Durnford D., Lehnherr I., Steffen A., and Morrison H. (2015) Atmospheric mercury in the Canadian Arctic. Part II: Insight from modelling, *Science of The Total Environment*, 509–510, 16-27, http://dx.doi.org/10.1016/j.scitotenv.2014.10.112.

De Simone F., Cinnirella S., Gencarelli C.N., Yang X., Hedgecock I.M., Pirrone N. (2015) Model Study of Global Mercury Deposition from Biomass Burning, *Environmental Science and Technology* 49 (11) 6712-6721.

De Simone F., Cinnirelli S., Gencarelli C.N., Carbone F., Hedgecock I.M., Pirrone N. (2016) Particulate-Phase Mercury Emissions during Biomass Burning and Impact on Resulting Deposition: a Modelling Assessment. *Atmos. Chem. Phys. Disc*., doi:10.5194/acp-2016-685 (under review).

De Simone F., Gencarelli C.N., Hedgecock I.M., and N. Pirrone (2016) A Modelling Comparison of Mercury Deposition from Current Anthropogenic Mercury Emission Inventories, *Environmental Science and Technology*, *50*(10), 5154–5162, doi:10.1021/acs.est.6b00691.

Deeds D.A., Banic C.M., Lu J., and Daggupaty S. (2013) Mercury speciation in a coal-fired power plant plume: An aircraft-based study of emissions from the 3640 MW Nanticoke Generating Station, Ontario, Canada, *Journal of Geophysical Research-Atmospheres*, 118, 4919-4935, 10.1002/jgrd.50349.

Demers J.D., Sherman L.S., Blum J.D., Marsik F.J. and Dvonch J.T. (2015) Coupling atmospheric mercury isotope ratios and meteorology to identify sources of mercury impacting a coastal urban-industrial region near Pensacola, Florida, USA, *Global Biogeochemical Cycles*, 29, 1689-1705, 10.1002/2015gb005146.

Denkenberger J.S., Driscoll C.T., Branfireun B.A., Eckley C.S., Cohen M. and Selvendiran P. (2012) A synthesis of rates and controls on elemental mercury evasion in the Great Lakes Basin, *Environmental Pollution*, 161, 291-298, 10.1016/j.envpol.2011.06.007.

Durnford D., Dastoor A., Ryzhkov A., Poissant L., Pilote M., and Figueras-Nieto D. (2012) How relevant is the deposition of mercury onto snowpacks? – Part 2: A modelling study, *Atmos. Chem. Phys*., 12, 9251-9274, 10.5194/acp-12-9251-2012.

Eckley C.S., Tate M.T., Lin C.J., Gustin M., Dent S., Eagles-Smith C., Lutz M.A., Wickland K.P., Wang B., Gray J.E., Edwards G.C., Krabbenhoft D.P., and Smith D.B. (2016) Surface-air mercury fluxes across Western North America: A synthesis of spatial trends and controlling variables, *Science of the Total Environment*, 568, 651-665, 10.1016/j.scitotenv.2016.02.121.

Fisher J.A., Jacob D.J., Soerensen A.L., Amos H.M., Corbitt E.S., Streets D.G., Wang Q., Yantosca R.M., Sunderland E.M. (2013) Factors driving mercury variability in the Arctic atmosphere and ocean over the past 30 years. *Global Biogeochemical Cycles* 27: 1226-1235.

Fisher J.A., Jacob D.J., Soerensen A.L., Amos H.M., Steffen A., and Sunderland E.M. (2012) Riverine source of Arctic Ocean mercury inferred from atmospheric observations, *Nature Geosci*, 5, 499-504.

Foy B. de, Y. Tong, X. Yin, W. Zhang, S. Kang, Q. Zhang, G. Zhang, X. Wang, and J. J. Schauer (2016) First field-based atmospheric observation of the reduction of reactive mercury driven by sunlight, *Atmospheric Environment*, *134* (March), 27–39, doi:10.1016/j.atmosenv.2016.03.028.

8921 Fu X., Yang X., Lang X., Zhou J., Zhang H., Yu B., Yan H., Lin C.-J., & Feng X. (2016) Atmospheric wet and litterfall mercury
8922 deposition at urban and rural sites in China, *Atmospheric Chemistry and Physics* 16(18), 11547--11562.
8923 Gencarelli C.N., Bieser J., Crabone F., De Simone F., Hedgecock I.M., Matthias V., Travnikov O., Yang X., Pirrone N. (2016)
8924 Sensitivity study of regional mercury dispersion in the atmosphere. *Atmos. Chem. Phys. Discuss.*, doi:10.5194/acp-
8925 2016-663 (under review).
8926 Gencarelli C.N., De Simone F., Hedgecock I.M., Sprovieri F., Pirrone N. (2014) Development and application of a regional-
8927 scale atmospheric mercury model based on WRF/Chem: a Mediterranean area investigation, *Environmental*
8928 *Science and Pollution Research* 21 (6), 4095-4109.
8929 Giang A., and Selin N.E. (2016) Benefits of mercury controls for the United States, Proceedings of the National Academy of
8930 Sciences of the United States of America, 113, 286-291, 10.1073/pnas.1514395113.
8931 Giang A., L.C. Stokes, D.G. Streets, E.S. Corbitt, and N.E. Selin (2015) Impacts of the Minamata Convention on Mercury
8932 Emissions and Global Deposition from Coal-Fired Power Generation in Asia, *Environmental Science & Technology*,
8933 *49*, 5236–5335, doi:10.1021/acs.est.5b00074.
8934 Goodsite M.E., Outridge P.M., Christensen J.H., Dastoor A., Muir D., Travnikov O., Wilson S. (2013) How well do
8935 environmental archives of atmospheric mercury deposition in the Arctic reproduce rates and trends depicted by
8936 atmospheric models and measurements? *Science of The Total Environment*, 452–453,196–207.
8937 Grant S.L., Kim M., Lin, P., Crist K.C., Ghosh S., and Kotamarthi V.R. (2014) A simulation study of atmospheric mercury and
8938 its deposition in the Great Lakes, *Atmospheric Environment*, 94, 164-172, 10.1016/j.atmosenv.2014.05.033.
8939 Gratz, L. E. et al. (2015), Oxidation of mercury by bromine in the subtropical Pacific free troposphere, *Geophysical Research*
8940 *Letters*, *42*(23), 10494–10502, doi:10.1002/2015GL066645.
8941 Gratz L.E., Ambrose J.L., Jaffe D.A., Knote C., Jaegle L., Selin N.E., Campos T., Flocke F.M., Reeves M., Stechman D., Steil M.,
8942 Weinheimer A.J., Knapp D.J., Montzka D.D., Tyndall G.S., Mauldin R.L., Cantrell C.A., Apel E.C., Hornbrook R.S., and
8943 Blake N.J. (2016) Airborne observations of mercury emissions from the Chicago/Gary urban/industrial area during
8944 the 2013 NOMADSS campaign, *Atmospheric Environment*, 145, 415-423, 10.1016/j.atmosenv.2016.09.051.
8945 Gratz L.E., Ambrose J.L., Jaffe D.A., Shah V., Jaegle L., Stutz J., Festa J., Spolaor M., Tsai C., Selin N.E., Song S., Zhou X.,
8946 Weinheimer A.J., Knapp D.J., Montzka D.D., Flocke F.M., Campos T.L., Apel E., Hornbrook R., Blake N.J., Hall S.,
8947 Tyndall G.S., Reeves M., Stechman D., and Stell M. (2015) Oxidation of mercury by bromine in the subtropical
8948 Pacific free troposphere, *Geophysical Research Letters*, 42, 10.1002/2015gl066645.
8949 Gratz L.E., Keeler G.J., Marsik F.J., Barres J.A., and Dvonch J.T. (2013a) Atmospheric transport of speciated mercury across
8950 southern Lake Michigan: Influence from emission sources in the Chicago/Gary urban area, *Science of the Total*
8951 *Environment*, 448, 84-95, 10.1016/j.scitotenv.2012.08.076.
8952 Gratz L.E., Keeler G.J., Morishita M., Barres J.A., and Dvonch J.T. (2013b) Assessing the emission sources of atmospheric
8953 mercury in wet deposition across Illinois, *Science of the Total Environment*, 448, 120-131,
8954 10.1016/j.scitotenv.2012.11.011.
8955 Gustin M.S., H.M. Amos, J. Huang, M.B. Miller, and K. Heidecorn (2015) Measuring and modelling mercury in the
8956 atmosphere: a critical review, *Atmospheric Chemistry and Physics*, *15*(10), 5697–5713, doi:10.5194/acp-15-5697-
8957 2015.
8958 Gustin M.S., Pierce A.M., Huang J., Miller M.B., Holmes H.A., and Loria-Salazar S.M. (2016) Evidence for Different Reactive
8959 Hg Sources and Chemical Compounds at Adjacent Valley and High Elevation Locations, *Environmental Science &*
8960 *Technology*, 50, 12225-12231, 10.1021/acs.est.6b03339.
8961 Gustin M.S., Amos H.M., Huang J., Miller M.B. & Heidecorn K. (2015) Measuring and modelling mercury in the atmosphere:
8962 a critical review, *Atmospheric Chemistry and Physics* **15**(10), 5697--5713.
8963 Hirdman D., Aspmo K., Burkhart J.F., Eckhardt S., Sodemann H., Stohl A. (2009) Transport of mercury in the Arctic
8964 atmosphere: evidence for a spring-time net sink and summer-time source. *Geophys Res Lett*; 36.
8965 http://dx.doi.org/10.1029/2009GL038345.
8966 Holmes C.D., Jacob D.J., Corbitt E.S., Mao J., Yang X., Talbot R., and Slemr F. (2010) Global atmospheric model for mercury
8967 including oxidation by bromine atoms, *Atmospheric Chemistry and Physics*, 10, 12037-12057.
8968 Holmes C.D., Krishnamurthy N.P., Caffrey J.M., Landing W.M., Edgerton E.S., Knapp K.R., and Nair U.S. (2016)
8969 Thunderstorms Increase Mercury Wet Deposition, *Environmental Science & Technology* 50(17), 9343-9350.
8970 Horowitz H.M., D.J. Jacob, H.M. Amos, D.G. Streets, and E.M. Sunderland (2014) Historical Mercury Releases from
8971 Commercial Products: Global Environmental Implications, *Environmental Science and Technology*, *48*, 10242–
8972 10250, doi:dx.doi.org/10.1021/es501337j.
8973 Horowitz H.M., Jacob D.J., Zhang Y., Dibble T.S., Slemr F., Amos H.M., Schmidt J.A., Corbitt E.S., Marais E.A., and Sunderland
8974 E.M. (2017) A new mechanism for atmospheric mercury redox chemistry: Implications for the global mercury
8975 budget, *Atmospheric Chemistry and Physics Discussions*, 1-33, doi:10.5194/acp-2016-1165.
8976 Huang J., and Gustin M.S. (2015) Use of Passive Sampling Methods and Models to Understand Sources of Mercury
8977 Deposition to High Elevation Sites in the Western United States, *Environmental Science & Technology*, 49, 432-
8978 441, 10.1021/es502836w.
8979 Huang J., Chang F.-C., Wang S., Han Y.-J., Castro M., Miller E., and Holsen T. M. (2013) Mercury wet deposition in the
8980 eastern United States: characteristics and scavenging ratios, *Environmental Science-Processes & Impacts,* 15,
8981 2321-2328, 10.1039/c3em00454f.
8982 Huang J., Miller M.B., Edgerton E., and Gustin M.S. (2016) Deciphering the Chemical Forms of Gaseous Oxidized Mercury in
8983 Florida, USA, *Atmos. Chem. Phys. Discuss.*, 1-26, 10.5194/acp-2016-725.

Hui M. et al. (2016) Mercury Flows in China and Global Drivers, *Environmental Science & Technology*, acs.est.6b04094, doi:10.1021/acs.est.6b04094.

IJC (2015) Atmospheric Deposition of Mercury in the Great Lakes Basin, International Joint Commission, Windsor, Ontario, 23p.

Jaffe D.A. et al. (2014) Progress on Understanding Atmospheric Mercury Hampered by Uncertain Measurements, *Environmental Science and Technology*, *48*, 7204–7206, doi:dx.doi.org/10.1021/es5026432.

Jiang Y., Cizdziel J.V., and Lu D. (2013) Temporal patterns of atmospheric mercury species in northern Mississippi during 2011-2012: Influence of sudden population swings, *Chemosphere*, 93, 1694-1700, 10.1016/j.chemosphere.2013.05.039.

Jiao Y. and Dibble T.S. (2015) Quality Structures, Vibrational Frequencies, and Thermochemistry of the Products of Reaction of BrHg• with NO2, HO2, ClO, BrO, and IO, *The Journal of Physical Chemistry A* **119**(42), 10502-10510.

Jiao Y. and Dibble T.S. (2017) First kinetic study of the atmospherically important reactions BrHg(radical dot) + NO2 and BrHg(radical dot) + HOO, *Phys. Chem. Chem. Phys.* **xx**, xx.

Kaulfus A.S., Nair U.S., Holmes C.D., and Landing W.M. (0), Mercury Wet Scavenging and Deposition Differences by Precipitation Type, *Environmental Science & Technology* **0**(ja), null.

Kocman D., M. Horvat, N. Pirrone, and S. Cinnirella (2013) Contribution of contaminated sites to the global mercury budget, *Environmental Research*, *125*, 160–170, doi:10.1016/j.envres.2012.12.011.

Kos G., Ryzhkov A., Dastoor A., Narayan J., Steffen A., Ariya P.A., and Zhang L. (2013) Evaluation of discrepancy between measured and modelled oxidized mercury species, *Atmospheric Chemistry and Physics*, 13, 4839-4863.

Kos G., Ryzhkov A., Dastoor A., Narayan J., Steffen A., Ariya P.A. and Zhang L. (2013) Evaluation of discrepancy between measured and modelled oxidized mercury species, *Atmospheric Chemistry and Physics*, 13, 4839-4863, 10.5194/acp-13-4839-2013.

Kwon S.Y. and N.E. Selin (2016) Uncertainties in Atmospheric Mercury Modelling for Policy Evaluation, *Current Pollution Reports*, doi:10.1007/s40726-016-0030-8.

Lamborg C.H., C.R. Hammerschmidt, K.L. Bowman, G.J. Swarr, K.M. Munson, D.C. Ohnemus, P.J. Lam, L.-E. Heimbürger, M.J.A. Rijkenberg, and M.A. Saito (2014) A global ocean inventory of anthropogenic mercury based on water column measurements, *Nature*, *512*(7512), 65–68, doi:10.1038/nature13563.

Lei H., D.J. Wuebbles, X.-Z. Liang, Z. Tao, S. Olsen, R. Artz, X. Ren, and M. Cohen (2014) Projections of atmospheric mercury levels and their effect on air quality in the United States, *Atmospheric Chemistry and Physics*, *14*(2), 783–795, doi:10.5194/acp-14-783-2014.

Lei H., Liang X.Z., Wuebbles D.J. and Tao Z. (2013) Model analyses of atmospheric mercury: present air quality and effects of transpacific transport on the United States, *Atmospheric Chemistry and Physics*, 13, 10807-10825, 10.5194/acp-13-10807-2013.

Lei H., Wuebbles D. J., Liang X.Z., Tao Z., Olsen S., Artz R., Ren X., and Cohen M. (2014) Projections of atmospheric mercury levels and their effect on air quality in the United States, *Atmospheric Chemistry and Physics*, 14, 783-795, 10.5194/acp-14-783-2014.

Lynam M.M., Dvonch J.T., Hall N.L., Morishita M., and Barres J.A. (2014) Spatial patterns in wet and dry deposition of atmospheric mercury and trace elements in central Illinois, USA, Environmental *Science and Pollution Research*, 21, 4032-4043, 10.1007/s11356-013-2011-4.

Megaritis A.G., Murphy B.N., Racherla P.N., Adams P.J., and Pandis S.N. (2014) Impact of climate change on mercury concentrations and deposition in the eastern United States, *Science of the Total Environment*, 487, 299-312, 10.1016/j.scitotenv.2014.03.084.

Moore C.W., Obrist D., Steffen A., Staebler R.M., Douglas T.A., Richter A., and Nghiem S.V. (2014) Convective forcing of mercury and ozone in the Arctic boundary layer induced by leads in sea ice, *Nature*, 506, 81-84, 10.1038/nature12924.

Muntean M., Janssens-Maenhout G., Song S., Selin N.E., Jos Oliver J.G.J., Guizzardi D., Maas R., Dentener F., (2014) Trend analysis from 1970 to 2008 and model evaluation of EDGARv4 global gridded anthropogenic mercury emissions. Science *of the Total Environment* 494-495, 337-350.

Myers T., Atkinson R.D., Bullock O.R., Jr., and Bash J.O. (2013) Investigation of effects of varying model inputs on mercury deposition estimates in the Southwest US, *Atmospheric Chemistry and Physics*, 13, 997-1009, 10.5194/acp-13-997-2013.

Nair U.S., Wu Y., Holmes C.D., Ter Schure A., Kallos G., and Walters J.T. (2013) Cloud-resolving simulations of mercury scavenging and deposition in thunderstorms, *Atmospheric Chemistry and Physics*, 13, 10143-10157, 10.5194/acp-13-10143-2013.

Outridge P., Macdonald R., Wang F., Stern G., Dastoor A. (2008) A mass balance inventory of mercury in the Arctic Ocean. *Environ. Chem.*, *5* (2), 89–111; DOI 10.1071/EN08002.

Pacyna J.M., Travnikov O., De Simone F., Hedgecock I.M., Sundseth K., Pacyna E.G., Steenhuisen F., Pirrone N., Munthe J., Kindbom K. (2016) Current and future levels of mercury atmospheric pollution on a global scale. *Atmos. Chem. Phys*. 16, 12495-12511. doi:10.5194/acp-16-12495-2016

Pirrone N., Cinnirella S., Feng X., Finkelman R.B., Friedli H.R., Leaner J., Mason R., Mukherjee A.B., Stracher G.B., Streets D.G., and Telmer K. (2010) Global mercury emissions to the atmosphere from anthropogenic and natural sources, *Atmospheric Chemistry and Physics*, 10, 5951-5964, 10.5194/acp-10-5951-2010.

Prestbo E.M., and Gay D.A. (2009) Wet deposition of mercury in the U.S. and Canada, 1996–2005: Results and analysis of the NADP mercury deposition network (MDN), *Atmospheric Environment*, 43, 4223-4233, http://dx.doi.org/10.1016/j.atmosenv.2009.05.028.

Rafaj P., Cofala J., Kuenen J., Wyrwa A., Zysk J. (2014) Benefits of European Climate Policies for Mercury Air Pollution, *Atmosphere* 5 (1), 45-59. doi:10.3390/atmos5010045.

Ren X., Luke W.T., Kelley P., Cohen M.D., Artz R., Olson M.L., Schmeltz D., Puchalski M., Goldberg D.L., Ring A., Mazzuca G.M., Cummings K.A., Wojdan L., Preaux S., and Stehr J.W. (2016) Atmospheric mercury measurements at a suburban site in the Mid-Atlantic United States: Inter-annual, seasonal and diurnal variations and source-receptor relationships, *Atmospheric Environment*, 146, 141-152 10.1016/j.atmosenv.2016.08.028.

Ren X., Luke W.T., Kelley P., Cohen M., Ngan F., Artz R., Walker J., Brooks S., Moore C., Swartzendruber P., Bauer D., Remeika J., Hynes A., Dibb J., Rolison J., Krishnamurthy N., Landing W.M., Hecobian A., Shook J., and Huey L.G. (2014) Mercury Speciation at a Coastal Site in the Northern Gulf of Mexico: Results from the Grand Bay Intensive Studies in Summer 2010 and Spring 2011, *Atmosphere*, 5, 230-251, 10.3390/atmos5020230.

Rolison J.M., Landing W.M., Luke W., Cohen M., and Salters V.J.M. (2013) Isotopic composition of species-specific atmospheric Hg in a coastal environment, *Chemical Geology*, 336, 37-49, 10.1016/j.chemgeo.2012.10.007.

Schroeder W.H. & Munthe J. (1998) Atmospheric mercury—An overview', *Atmospheric Environment* 32(5), 809 - 822.

Selin N.E. (2014) Global change and mercury cycling: challenges for implementing a global mercury treaty, *Environmental Toxicology and Chemistry*, *33*(6), 1202–10, doi:10.1002/etc.2374.

Selin N.E., Jacob D.J., Park R.J., Yantosca R.M., Strode S., Jaegle L., and Jaffe D. (2007) Chemical cycling and deposition of atmospheric mercury: Global constraints from observations, *Journal of Geophysical Research-Atmospheres,* 112, 10.1029/2006jd007450.

Shah V., Jaegle L., Gratz L.E., Ambrose J.L., Jaffe D.A., Selin N.E., Song S., Campos T.L., Flocke F.M., Reeves M., Stechman D., Stell M., Festa J., Stutz J., Weinheimer A.J., Knapp D.J., Montzka D.D., Tyndall G.S., Apel E.C., Hornbrook R.S., Hills A.J., Riemer D.D., Blake N.J., Cantrell C.A., and Mauldin R.L. (2016) Origin of oxidized mercury in the summertime free troposphere over the southeastern US, *Atmospheric Chemistry and Physics,* 16, 1511-1530, 10.5194/acp-16-1511-2016.

Sommar J., M.E. Andersson, and H.W. Jacobi (2010) Circumpolar measurements of speciated mercury, ozone and carbon monoxide in the boundary layer of the Arctic Ocean, *Atmos. Chem. Phys*., 10(11), 5031–5045.

Song S., Selin N.E., Soerensen A.L., Angot H., Artz R., Brooks S., Brunke E.G., Conley G., Dommergue A., Ebinghaus R., Holsen T.M., Jaffe D.A., Kang S., Kelley P., Luke W.T., Magand O., Marumoto K., Pfaffhuber K.A., Ren X., Sheu G.R., Slemr F., Warneke T., Weigelt A., Weiss-Penzias P., Wip D.C., and Zhang Q. (2015) Top-down contents on atmospheric mercury emissions and implications for global biogeochemical cycling, *Atmos. Chem. Phys*., 15, 7103-7125.

Steffen A., Bottenheim J., Cole A., Ebinghaus R., Lawson G. and Leaitch W.R. (2014) Atmospheric mercury speciation and mercury in snow over time at Alert, Canada, *Atmospheric Chemistry and Physics*, 14, 2219-2231.

Steffen A., Schroeder W., Macdonald R., Poissant L., and Konoplev A. (2005) Mercury in the Arctic atmosphere: An analysis of eight years of measurements of GEM at Alert (Canada) and a comparison with observations at Amderma (Russia) and Kuujjuarapik (Canada), *Science of The Total Environment*, 342, 185-198, http://dx.doi.org/10.1016/j.scitotenv.2004.12.048.

Stein A.F., Draxler R.R., Rolph G.D., Stunder B.J.B., Cohen M.D., and Ngan F. (2015) NOAA's HYSPLIT atmospheric transport and dispersion modelling system, Bulletin of the American Meteorological Society, 10.1175/BAMS-D-14-00110.1.

Stern G.A., Macdonald R.W., Outridge P.M., Wilson S., Chételat J., Cole A., Hintelmann H., Loseto L.L., Steffen A., Wang F., Zdanowicz C. (2012) How does climate change influence Arctic mercury? *Sci Total Environ*.; 414:22-42. doi: 10.1016/j.scitotenv.2011.10.039.

Streets D.G., M.K. Devane, Z.F. Lu, T.C. Bond, E.M. Sunderland, and D.J. Jacob (2011) All-time releases of mercury to the atmosphere from human activities, *Environ. Sci. Technol.*, 45(24), 10, 485–10,491, doi:10.1021/es202765m.

Sunderland E.M., and N.E. Selin (2013) Future trends in environmental mercury concentrations: implications for prevention strategies., *Environmental health : a global access science source*, *12*, 2, doi:10.1186/1476-069X-12-2.

Sunderland E.M., Driscoll C.T., Hammitt J.K., Grandjean P., Evans J.S., Blum J.D., Chen C.Y., Evers D.C., Jaffe D.A., Mason R.P., Goho S., and Jacobs W. (2016) Benefits of Regulating Hazardous Air Pollutants from Coal and Oil Fired Utilities in the United States, *Environmental Science & Technology*, 50, 2117-2120, 10.1021/acs.est.6b00239.

Toyota K., Dastoor A.P., and Ryzhkov A. (2014) Air–snowpack exchange of bromine, ozone and mercury in the springtime Arctic simulated by the 1-D model PHANTAS – Part 2: Mercury and its speciation, Atmos. Chem. Phys., 14, 4135-4167, doi:10.5194/acp-14-4135-2014.

Toyota K., Dastoor A.P., and Ryzhkov, A. (2016) Parameterization of gaseous dry deposition in atmospheric chemistry models: Sensitivity to aerodynamic resistance formulations under statically stable conditions, *Atmospheric Environment* 147, 409 - 422.

Travnikov O. and I. Ilyin (2009) The EMEP/MSC-E mercury modelling system. In: Pirrone N, Mason RP, editors. Mercury Fate and Transport in the Global Atmosphere. Dordecht: *Springer*. pp. 571−587.

Travnikov O., Angot H., Artaxo P., Bencardino M., Bieser J., D'Amore F., Dastoor A., De Simone F., Diéguez M. D. C., Dommergue A., Ebinghaus R., Feng X. B., Gencarelli C. N., Hedgecock I. M., Magand O., Martin L., Matthias V., Mashyanov N., Pirrone N., Ramachandran R., Read K. A., Ryjkov A., Selin N. E., Sena F., Song S., Sprovieri F., Wip D., Wängberg I., and Yang X. (2017) Multi-model study of mercury dispersion in the atmosphere: atmospheric processes and model evaluation, Atmos. Chem. Phys., 17, 5271-5295, doi:10.5194/acp-17-5271-2017.

UNEP (2015) Global Mercury Modelling: Update of Modelling Results in the Global Mercury Assessment 2013.

Velasco A., Arcega-Cabrera F., Oceguera-Vargas I., Ramirez M., Ortinez A., Umlauf G., and Sena F. (2016) Global Mercury Observatory System (GMOS): measurements of atmospheric mercury in Celestun, Yucatan, Mexico during 2012, *Environmental Science and Pollution Research*, 23, 17474-17483, 10.1007/s11356-016-6852-5.

Wang F., A. Saiz-Lopez, A.S. Mahajan, J.C. Gómez Martín, D. Armstrong, M. Lemes, T. Hay, and C. Prados-Roman (2014a) Enhanced production of oxidised mercury over the tropical Pacific Ocean: a key missing oxidation pathway, *Atmospheric Chemistry and Physics*, *14*(3), 1323–1335, doi:10.5194/acp-14-1323-2014.

Wang L., S. Wang, L. Zhang, Y. Wang, Y. Zhang, C. Nielsen, M. B. McElroy, and J. Hao (2014b), Source apportionment of atmospheric mercury pollution in China using the GEOS-Chem model, *Environmental Pollution*, *190*, 166–175, doi:10.1016/j.envpol.2014.03.011.

Wang X., Z. Bao, C. J. Lin, W. Yuan, and X. Feng (2016), Assessment of Global Mercury Deposition through Litterfall. *Environmental Science and Technology*, *50*(16), 8548–8557, doi:10.1021/acs.est.5b06351.

Weigelt A., Slemr F., Ebinghaus R., Pirrone N., Bieser J., Bödewadt J., Esposito G., Van Velthoven P. (2016) Mercury emissions of a coal fired power plant in Germany. *Atmos. Chem. Phys*. 16, 13653-13668. doi: 10.5194/acp-16-13653-2016

Weiss-Penzias P., Amos H.M., Selin N.E., Gustin M.S., Jaffe D.A., Obrist D., Sheu G.R., and Giang A. (2015) Use of a global model to understand speciated atmospheric mercury observations at five high-elevation sites, *Atmospheric Chemistry and Physics*, 15(3), 1161-1173, 10.5194/acp-15-1161-2015.

White E.M., Landis M.S., Keeler G.J., and Barres J.A. (2013) Investigation of mercury wet deposition physicochemistry in the Ohio River Valley through automated sequential sampling, *Science of the Total Environment*, 448, 107-119, 10.1016/j.scitotenv.2012.12.046.

Wright G., Gustin M.S., Weiss-Penzias P., and Miller M.B. (2014) Investigation of mercury deposition and potential sources at six sites from the Pacific Coast to the Great Basin, USA, *Science of the Total Environment*, 470, 1099-1113, 10.1016/j.scitotenv.2013.10.071.

Wright L.P., and Zhang L. (2015) An approach estimating bidirectional air-surface exchange for gaseous elemental mercury at AMNet sites, *Journal of Advances in Modelling Earth Systems*, 7, 35-49, 10.1002/2014ms000367.

Wright L.P., Zhang L., and Marsik F.J. (2016) Overview of mercury dry deposition, litterfall, and throughfall studies, *Atmospheric Chemistry and Physics* 16(21), 13399--13416.

Wu Q., Wang S., Li G., Liang S., Lin C.-J., Wang Y., Cai S., Liu K., and Hao J. (2016) Temporal Trend and Spatial Distribution of Speciated Atmospheric Mercury Emissions in China During 1978–2014, *Environmental Science & Technology* 50(24), 13428-13435.

Xu X.H., Akhtar U., Clark K., and Wang X.B. (2014) Temporal Variability of Atmospheric Total Gaseous Mercury in Windsor, ON, Canada, *Atmosphere*, 5, 536-556, 10.3390/atmos5030536.

Zhang H., C.D. Holmes and S. Wu (2016a), Impacts of changes in climate, land use and land cover on atmospheric mercury, *Atmospheric Environment*, *141*, 230–244, doi:10.1016/j.atmosenv.2016.06.056.

Zhang L., Blanchard P., Johnson D., Dastoor A., Ryzhkov A., Lin C.J., Vijayaraghavan K., Gay D., Holsen T.M., Huang J., Graydon J.A., St Louis V.L., Castro M.S., Miller E.K., Marsik F., Lu J., Poissant L., Pilote M., and Zhang K.M. (2012) Assessment of modelled mercury dry deposition over the Great Lakes region, *Environmental Pollution*, 161, 272-283, 10.1016/j.envpol.2011.06.003.

Zhang L., Wu Z., Cheng I., Wright L.P., Olson M.L., Gay D.A., Risch M.R., Brooks S., Castro M.S., Conley G.D., Edgerton E.S., Holsen T.M., Luke W., Tordon R., and Weiss-Penzias P. (2016) The Estimated Six-Year Mercury Dry Deposition Across North America, *Environmental Science & Technology*, 10.1021/acs.est.6b04276.

Zhang Y.X. and Jaegle L. (2013) Decreases in Mercury Wet Deposition over the United States during 2004-2010: Roles of Domestic and Global Background Emission Reductions, *Atmosphere*, 4, 113-131, 10.3390/atmos4020113.

Zhang Y., D.J. Jacob, H.M. Horowitz, L. Chen, H.M. Amos, D.P. Krabbenhoft, F. Slemr, V.L. St Louis, and E.M. Sunderland (2016b) Observed decrease in atmospheric mercury explained by global decline in anthropogenic emissions, *Proceedings of the National Academy of Sciences of the United States of America*, *113*(3), 526–31, doi:10.1073/pnas.1516312113.

Zhang Y., D.J. Jacob, S. Dutkiewicz, H.M. Amos, M.S. Long, and E.M. Sunderland (2015) Biogeochemical drivers of the fate of riverine mercury discharged to the global and Arctic oceans, *Global Biogeochem. Cycles*, 29, 854–864, doi:10.1002/2015GB005124.

Zhang Y., L. Jaeglé, L. Thompson, and D.G. Streets (2014) Six centuries of changing oceanic mercury, *Global Biogeochemical Cycles*, *28*(11), 1251–1261, doi:10.1002/2014GB004939.

Zhang Y., Jacob D.J., Horowitz H.M., Chen L., Amos H.M., Krabbenhoft D.P., Slemr F., St. Louis, V.L., and Sunderland E.M. (2016) Observed decrease in atmospheric mercury explained by global decline in anthropogenic emissions, *Proceedings of the National Academy of Sciences* 113(3), 526-531.

Zhou H., Zhou C., Lynam M.M., Dvonch J.T., Barres J.A., Hopke P.K., Cohen M. and Holsen T.M. (2016) Atmospheric Mercury Temporal Trends in the Northeastern United States from 1992 to 2014: Are Measured Concentrations Responding to Decreasing Regional Emissions?, *Environmental Science and Technology Letters*, (submitted).

Zhu J., Wang T., Bieser J., Matthias V. (2015) Source attribution and process analysis for atmospheric mercury in eastern China simulated by CMAQ-Hg. *Atmos. Chem. Phys*. 5 (15).

9170

9171